NAS 8-11235

QUARTERLY REPORT

MICROELECTRONICS RESEARCH ON

SILICON-SiLICON OXIDE

STRUCTURES AND INTERFACES

NOVEMBER 30, 1964

Submitted to

GEORGE C. MARSHALL SPACE FLIGHT CENTER

NATIONAL AERONAUTICS AND SPACE ADMINISTRATION
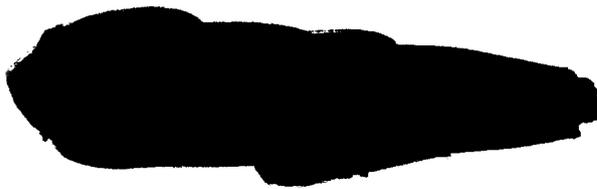
by

THE ELECTRONIC MATERIALS RESEARCH LABORATORY
THE UNIVERSITY OF TEXAS
AUSTIN, TEXAS 78712

NAS 8-11235
Quarterly Report Summary
Microelectronics Research on Silicon-
Silicon Oxide Structures and Interfaces

Summary   33170

The development of capability towards satisfactory completion of
the program continues. Some of the considerable recently-published
information on M-O-S structures is reviewed. A major point of agreement
on space charge in the oxide has been reached. Significant details are
yet to be explained.

The experimental program now has operating the process furnace,
the electrolytic etching fixture, the capacitance bridge, the replication
evaporator, and the electron microscope. The deionized water system
produces 18 meg ohm-centimeter water. Simple usage of photolithographic
techniques has been satisfactorily demonstrated. The necessary laboratory
operations can now be executed.

Fluorescence techniques appear to offer a sensitive analytical tool
for measuring the organic content in deionized water supplies. Investi-
gations to evaluate the utility of the techniques can be performed with
additional equipment. Electron mirror microscopy appears to need further
development to have the resolution desired for cross section investigations.
For studying the uniformity and structure of oxide surfaces this tool
could be quite useful.

New general bibliography sections cover report literature recently
surveyed.

TABLE OF CONTENTS

Microelectronics Research on
Silicon-Silicon Oxide Structures and Interfaces

LIST OF FIGURES

Contract NAS 8-11235
Second Quarterly Report
for the Period 1 September to 30 November 1964

MICROELECTRONICS RESEARCH ON
SILICON-SILICON OXIDE STRUCTURES AND INTERFACES

I. Models of Oxide Structures

    A. Physical Model of the M-O-S Device

Figure 1
Cross Section of M-O-S Structure

Consider the case when the metal is biased positive with respect to the n-type semiconductor. There will be positive charges at the metal-oxide interface and electrons at the silicon-silicon oxide interface. The result is that there will be an accumulation region in the silicon (particularly at the silicon-oxide interface).

The measured capacitance will be that of the oxide and is given by the expression

$$C_O = \frac{\varepsilon_1 S}{X_O} \tag{1}$$

where ε_1 is the permittivity of the oxide, S is the cross sectional area of the device, and X_O is the width of the oxide layer.

Next consider the case when the metal is biased negative with respect to the semiconductor. Electrons will be transported from the semiconductor to the metal leaving exposed impurity ions in the semicon-

ductor thus creating a space charge region. By the condition of charge neutrality the total charge in the depletion region is equal to the charge on the metal plate. This value is given by

$$Q = CV \tag{2}$$

where C is the measured capacitance of the device and V is the voltage drop across it.

This is equivalent to a parallel plate capacitor with two dielectrics between the plates as in Figure 2 where d_1 is the dielectric number one, the oxide, and d_2 is the dielectric number two, the semiconductor.
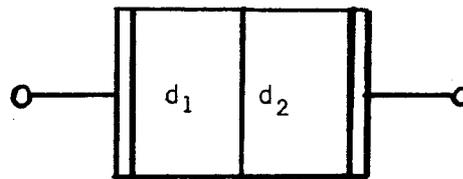
Figure 2
Two Dielectric Capacitor

The capacitance for this configuration is

$$C = \frac{C_1 C_2}{C_1 + C_2} \tag{3}$$

where

$$C_1 = \frac{\varepsilon_1 S}{X_1} \quad , \qquad C_2 = \frac{\varepsilon_2 S}{(X_2 - X_1)}$$

The M-O-S device can therefore be represented as two capacitors in series as in Figure 3. One capacitor is due to the oxide layer and is constant; the other is due to the depletion region and is a function of bias.
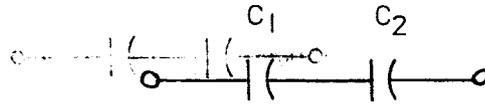
Figure 3
Capacitors in Series

For the purpose of this derivation it will be assumed that the capacitance vs. voltage curve for the device is available from measurements made on the device. The capacitance will be the series equivalent of the two capacitors and the voltage will be the total barrier voltage. The capacitance due to the depletion region can be found from the expression

$$C_d = \frac{C_o C}{C_o - C} \tag{4}$$

The total voltage is the sum of the drops across the two capacitors, the contact potential, and the IR drop

$$V_t = V_o + V_d + V_c + IR \tag{5}$$

where

V_t = applied voltage

V_o = oxide voltage drop

V_d = depletion layer voltage drop

V_c = contact potential

IR = drop due to leakage current.

The leakage current I will be measured but its value will probably be such that it can be neglected. It is hoped that the contact potential can be determined during the course of this work; however, for the present this

will be neglected or a constant assumed (on the order of 0.5 volts). The simplified voltage is now

$$V_t = V_o + V_d \qquad (6)$$

The voltage drop can be determined in the following manner:

$$Q_T = Q_o = Q_d \qquad (7)$$

This is equivalent to saying that the charge is the same on all plates of the capacitor.

$$CV = C_o V_o = C_d V_d \qquad (8)$$

$$\frac{C_o C_d}{C_o + C_d} (V_o + V_d) = C_o V_o = C_d V_d$$

$$V_d = \frac{C_o V}{C_o + C_d} \qquad (9)$$

Thus, the capacitance of the depletion region and the voltage drop across it can be determined from the voltage vs. capacitance curve.

If a small reverse bias is applied to the device the depletion region formed will be narrow. For this region the charge density can be assumed to be constant. The plot of charge density vs. distance for this condition is shown in Figure 5. X_{d_1} is the depletion width of this small bias.
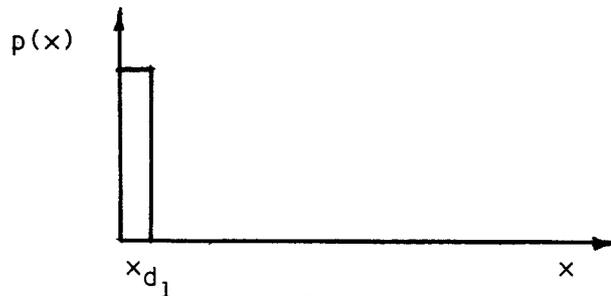
Figure 4a
Charge Density Versus Distance

Assuming the charge density varies only with X (one dimensional case), the relationship can be expressed as

$$Q_{d_1} = p_1(x)X_{d_1} \tag{10}$$

thus, both the charge density and the depletion width can be obtained from the C vs. V curve.

Next the bias is increased by a small amount. This results in more charge being uncovered and the widening of the depletion region.
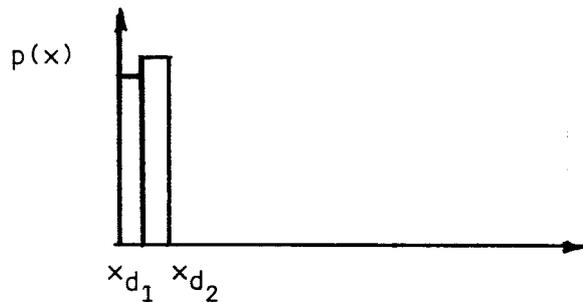
Figure 4b
Charge Density Versus Distance

The situation might be that of Figure 6. The depletion width is given by

$$C_{d_2} = \frac{\varepsilon S}{X_{d_2}} \tag{11}$$

and the charge is given by

$$Q_{d_2} = C_{d_2} V_{d_2} = p_1(x)X_{d_1} + p_2(x)(x_{d_2} - x_{d_1}) \tag{12}$$

thus, the charge density can be determined as well as the depletion region.

The bias is now increased slightly and the process is repeated. This is done until a complete curve of charge density vs. distance is obtained.
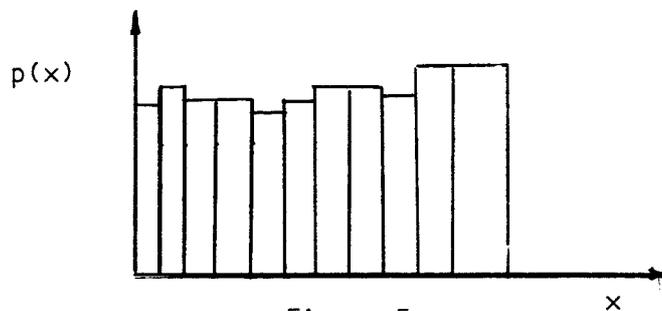
Figure 5
Histogram of Charge Density Versus Distance

In a depletion region the charge density is given by

$$p(x) = e[N_d - N_a] \qquad (13)$$

where

e = charge on the electron

N_d = donor impurity concentration

N_a = Acceptor impurity concentration

Thus, the impurity profile can be calculated from the charge density curve.

B. Recent Publications on M-O-S Structures

During the last several months there have been several papers published on the M-O-S device. A large number of these papers have been written by scientists with the IBM Corporation[1] and with Fairchild Semiconductor.[2] One of the major results of their studies has been to determine that the ions can migrate throughout the oxide of the M-O-S device and create a space charge in the oxide. The ions are thought to be oxygen vacancies in the case of the Si-SiO$_2$ system. Use of a model based on oxygen ion vacancy migration can be used to explain some of the major phenomena of M-O-S devices while other phenomena can be explained only with a surface state model. Other phenomena are yet to be explained. At the present understanding of the M-O-S device, a model which uses both the

surface state and ion migration phenomena gives the most complete picture.
A review of the models follows.

Due to the abrupt change from a periodic crystal lattice at the
surface of a semiconductor, energy states exist for carriers that are not
allowed in the bulk of the material. These states in the surface state
model may trap carriers and as a consequence the surface can become
changed. A method for determining the charges trapped in surface states
is shown below in Figure 6.
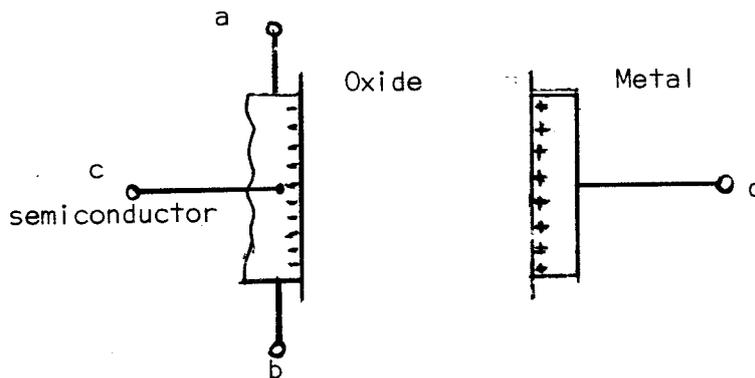
Figure 6
Conductance Electrode M-O-S Structure

The bias between points c and d can be varied thus changing the
charge at the metal oxide interface and at the semiconductor oxide inter-
face. The charge at the semiconductor-oxide interface will result in a
change in the conduction between points a and b. If the mobility of the
charge carriers is known, the theoretical change in conduction between
points a and b may be calculated. In practice the change in conductivity
is not usually the theoretical value but lower and a function of frequency.
The explanation most used is that of the surface states. If a low frequency

signal is used to modulate the conductivity between a and b, the states are filled and emptied as the signal varies. Since the situation is that of steady state the maximum number of surface states would be filled (maximum number of carriers trapped) and the conductivity change between "a" and "b" would be a minimum.

If the frequency of the signal between "c" and "d" is increased, some of the states will not be filled due to insufficient time. In this case there will be more carriers to conduct current between "a" and "b" and the change in conductivity between these points would be higher than in the previous case. If the frequency is further increased, the conductivity change will increase until at some high frequency none of the surface states will be filled and the change in conductivity between "a" and "b" will be a maximum for the applied signal between "c" and "d". Another way of demonstrating this effect would be to apply a negative step voltage at point "c". The conductivity would change immediately by an amount corresponding to there being no surface states but would then decay exponentially as the surface states were filled to some value corresponding to the situation of all of the surface states being filled. This is shown in Figure 7. The step voltage is applied at t = 0.
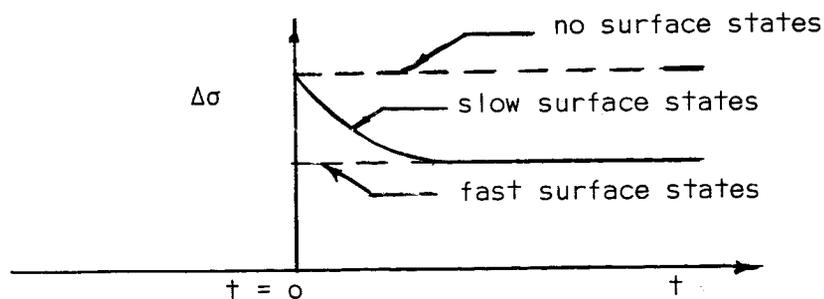
Figure 7
Idealized Charge-Conductivity-Time Relationship

-8-

If the step voltage is left at "c" for an extended time the conductivity is noted to decrease still further. This would seem to correspond to filling of extremely slow surface states. The experiment may have to be conducted at elevated temperatures to observe this secondary effect but since the filling and emptying of surface states is a function of temperature, this is not unreasonable. However, when the step voltage is removed the conductivity changes to a value below its original value and the conductivity is stable at this point. This case is shown in Figure 8.
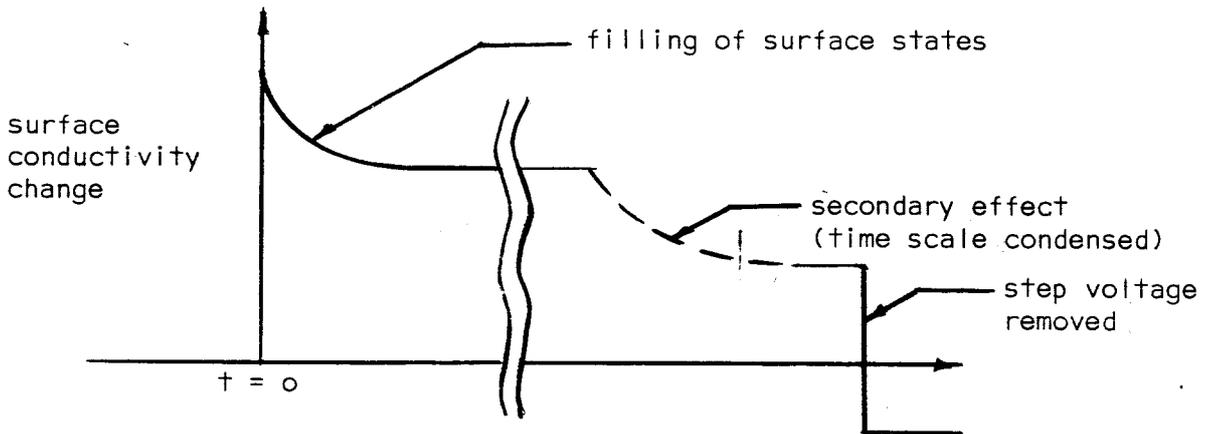
Figure 8
Observed Charge-Conductivity-Time Relationship

The secondary effect has been explained in the following manner. During the time when the step voltage is applied to point "c", ions in the oxide layer migrate to the semiconductor-oxide interface (especially if the experiment is conducted at higher temperatures). These ions tend to pile up at the interface. The arrangement is semipermanent, thus creating a significant space charge field within the oxide. When the step voltage is

removed from point "c" the space charge remains.

In the case of the $Si-SiO_2$ system the ions in the oxide are thought to be oxygen vacancies. This tends to be supported by the fact that the space charge is usually positive and that the presence of an oxidizing agent tends to stabilize the effect while the presence of a reducing agent aggravates it. The oxidizing agent is thought to be a source of oxygen to fill the vacancies and the reducing agent is thought to capture some of the oxygen from the SiO_2. In the experiments reported, aluminum was the metal used to make the contact with the silicon-dioxide and it is thought that the oxygen in the oxide can react with the aluminum thus creating the vacancies. The vacancies, once created, are able to migrate throughout the oxide under the influence of an electric field and/or temperature.

This model of contact-metal-caused vacancies can be used to explain some of the phenomena associated with the M-O-S structure. One of the phenomena is that the M-O-S structure can be considered as a diode with the ion current flow 100 times or more greater in one direction than when biased in the following direction.

If the metal is biased negative, oxygen ions will be forced to the $Si-SiO_2$ interface under the influence of the field. However, since the ions can only migrate if vacancies exist and the vacancies are assumed to be formed at the aluminum-oxide interface there will be little current flow due to the fact that the silicon-oxide is saturated a little ways from the metal. If the metal is now biased positive, oxygen ions will be attracted to it thus letting the vacancies migrate toward the silicon.

-10-

Since the oxygen is assumed to react with the metal, vacancies can be formed at the metal-oxide interface and the process can continue. The current will be much larger in this case. The space charge created with the metal biased positive will be large.

The space charge in the oxide can be studied by measuring the capacitance versus voltage of the M-O-S device. Theoretical curves of capacitance versus voltage can be calculated where the applied voltage V_{app} is equal to

$$V_{app} = \phi_{ms} + \frac{Q_{ss}}{C_o} \tag{14}$$

where ϕ_{ms} is the work function difference between the metal and semiconductor and Q_{ss} is charge density of the surface states. If there is a space charge in the oxide, an additional term represents its effect on the potential.

$$V_{app} = \phi_{ms} + \frac{Q_{ss}}{C_o} + \frac{1}{X_o C_o}\int_o^{X_o} xp(x)dx \tag{15}$$

The term $\int_o^{X_o}\frac{1}{X_o C_o} xp(x)dx$ corresponds to an effective charge located at the Si-SiO$_2$ interface. The terms represent a horizontal shift of the C versus V curves. If the C versus V curve can be obtained without a space change and then with a space charge the amount of charge in the oxide can be determined.
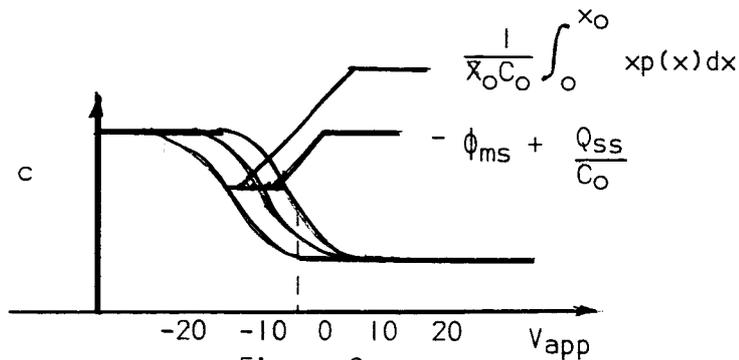
Figure 9
High Frequency Capacitance Versus Voltage

In summary, ion migration is probably one of the major phenomena occurring in the M-O-S device. However, there are aspects of this phenomenon which are not well understood. For instance, in some cases the space charge in the oxide appears to be negative rather than positive. The charge could not be oxygen ion vacancies in this case of course. The space charge model does not replace the surface state model but supplements it. There are phenomena which can only be explained by the surface state explanation. The space charge phenomena go a long way in helping to understand the M-O-S structure but there must be further study before complete understanding is achieved.

II.   Process Furnace Arrangement

The connection unit was built for the purpose of removing impurities from the gases used with the furnace, to provide a means of mixing the gases, and to provide a means of introducing steam to the gases.

Since the primary reason for the unit is to purify the gases, care must be exercised so that no impurities are added by the connection unit itself. For this reason inert materials were used throughout the system. Stainless steel, teflon, and quartz are the only materials used. All of the pipes and fittings are of stainless steel, the stoppers and O-rings are made of teflon, and the furnace tube and all flasks are quartz. This system will provide little contamination of the gases and help to provide for repro-ducibility of results.

The gas to be used in the oxidation process is bought in cylinders. Each cylinder is connected to a flow meter which allows the flow rate to be con-trolled. The gas flows from the flow meter to the input unit.

The input unit provides for the selection of gas and the mixing of gases if required. At present only two gases can be used; however, the system can be expanded to provide for three and more gases with a minimum of effort.

From the input unit the gas flows into the cold trap. The cold trap consists of a quartz flask sitting in liquid nitrogen. The gas flows into the cold trap and is delayed by a pyrex wool bundle long enough for the water vapor and other impurities which have a boiling point higher than nitrogen to condense and remain in the flask.

The gas then leaves the cold trap and goes into the furnace. Between the cold trap and the furnace a steam source can introduce steam into the gas.

This is optional and is controlled by a valve. The steam source is a quartz flask filled with deionized water and sitting in a heater which controls the temperature of the water.

There are several glass to metal connections in the system and since the materials were restricted to stainless steel, teflon, and quartz, special clamps had to be designed and built for these connections. The connections occur at the entrance to the furnace tube, the cold trap, and the steam source.

The most difficult connection was at the entrance to the furnace tube. The quartz furnace tube has an outside diameter of approximately two and one-half inches. The connection had to be easy to connect and remove because the arrangement of the furnace in the lab is such that the specimens have to be entered from the same end as the gas and the thermocouple used to profile the furnace. Figure 10 presents the design. The connector slips over the end of the quartz furnace tube and is then tightened. This compresses the teflon O-ring which makes a pressure contact with the quartz tube. The connector is of stainless steel. The upper rod extending from the end of the connector is for the gas input and the lower rod is for the thermocouple.

The connectors for the two flasks are similar to each other. The difference is that two rods extend into the flask for the cold trap and only one for the steam source. The connector consists of a teflon stopper with a hole for the stainless steel tubing to enter. The aluminum neck on the flask allows tightening of the stopper. The arrangement is shown in Figure 10.

Furnace

Mixer

Cold Trap

Input Unit

Water
Boiler

Optional

Flow Meter

Regulator

Gas Bottle
No. 1

Flow Meter

Regulator

Gas Bottle
No. 2
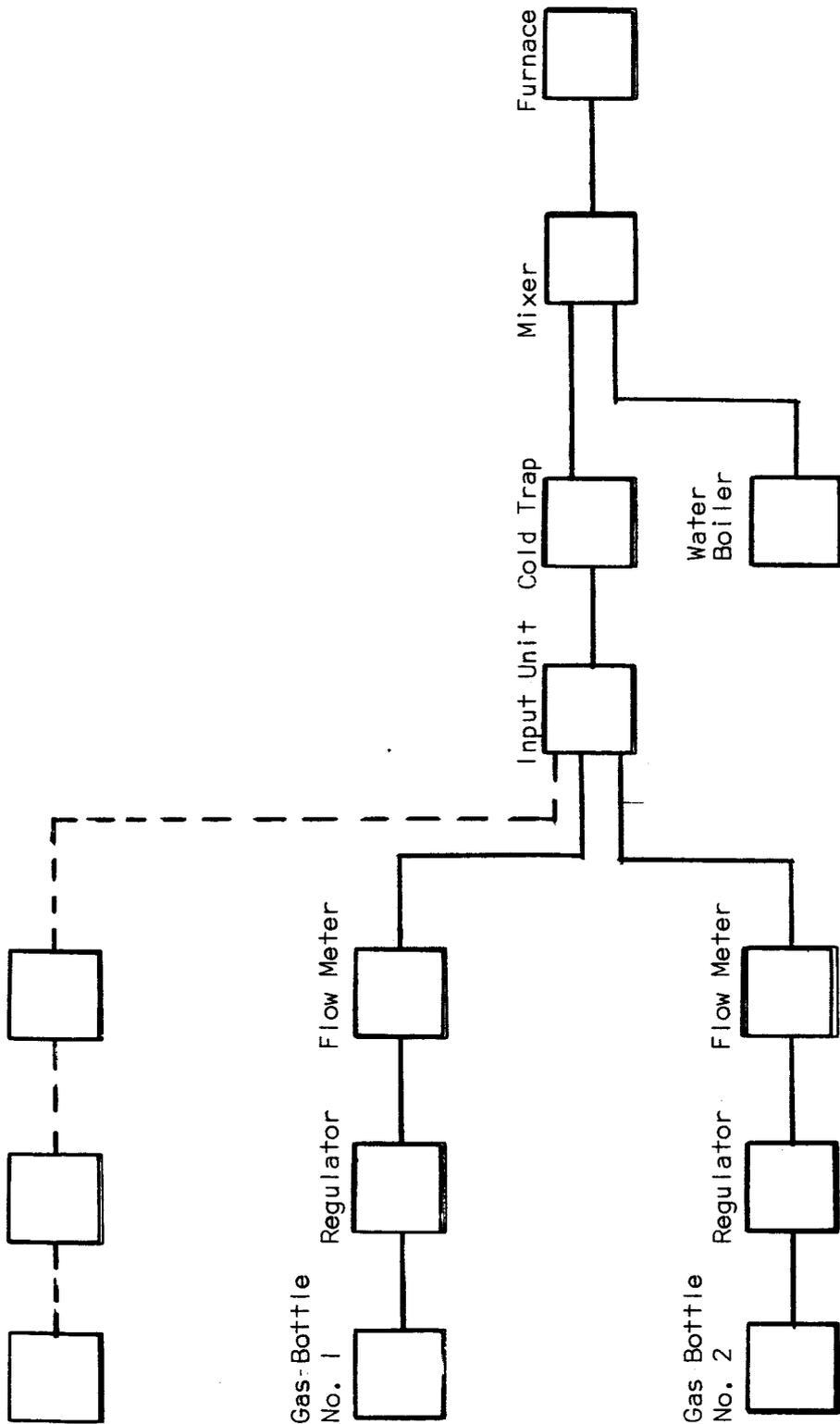
Figure 10a
Process Furnace Arrangement

Teflon

Stainless Steel

Aluminum

Flask Arrangement

Teflon
O-ring

Gas

Thermocouple
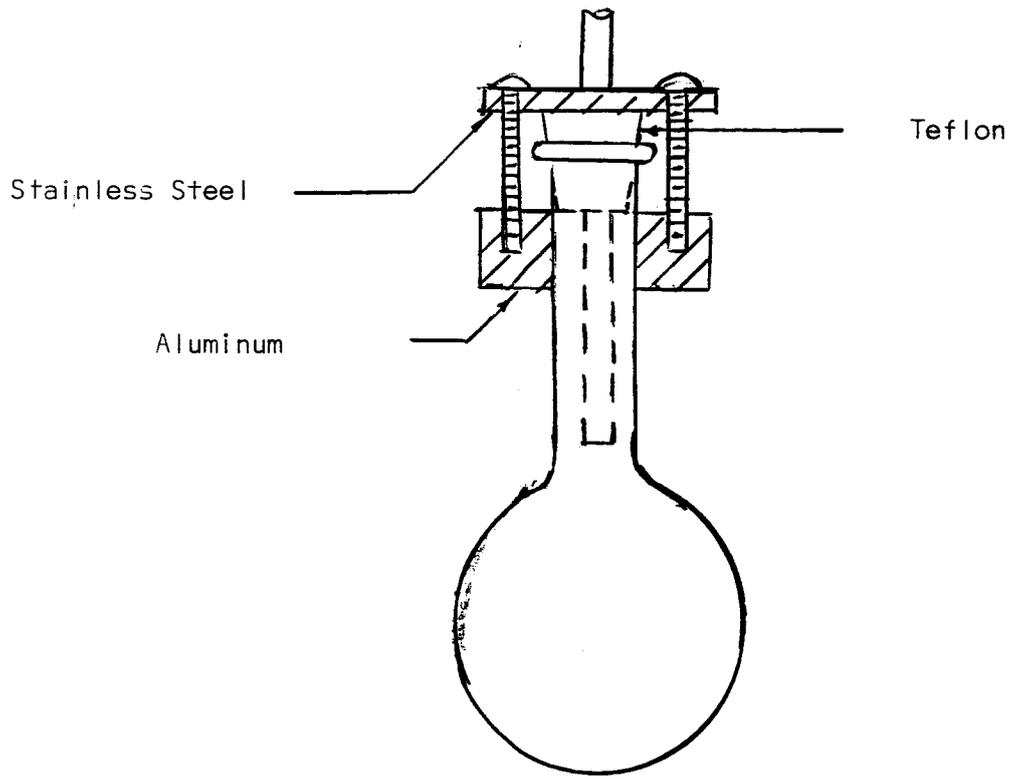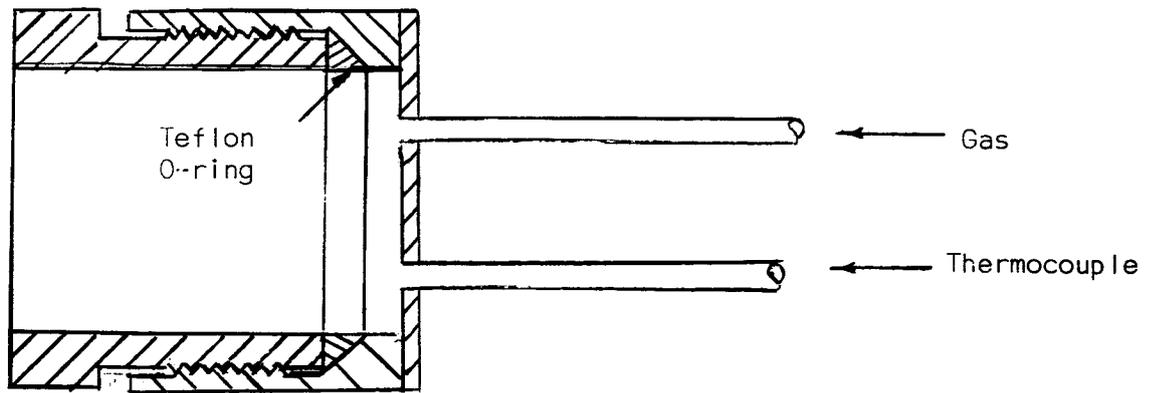
End Piece for Furnace Tube

Figure 10b

III. Capacitance Measurement

A.   Introduction

Experiments as early as 1746 at the University of Leyden indicated that electrical charge could be stored in a device later called a Leyden jar.[3] This device is the same, in principle, as a modern capacitor. Today, capacitors come in many configurations yet they follow the same physical laws as the early Leyden jar.

Capacitance relates charge to applied voltage. The amount of charge (q) stored in a capacitor is directly proportional to the potential difference (v) applied to the terminals of the device. In equation form:

$$q = Cv \tag{16}$$

where C, the constant of proportionality, is called the capacitance of the device. This defining relation holds for all configurations of capacitors.

We restrict ourselves to devices which relate current and the first derivative of voltage by a positive, real time invariant constant as in equation (2).[4]

$$i = C \frac{dv}{dt} \tag{17}$$

where C is the constant described above. The capacitors under discussion are properly described this way.

For such a device, it is possible to measure the value of the constant C in equations 1 and 2 to several significant figures. The degree of accuracy of measurement is dependent on the method of measurement and the internal accuracy of the measurement device.

Measurements of this type require both accuracy and precision. Accuracy refers to how close a measurement has been to the true value of a

quantity. Precision refers to the clustering of measurements around an average. Thus it can be seen that a measurement can fall either close or further away from its true value for high and low accuracy and successive measurements of the same quantity can show a small or large deviation about their average for high and low precision. The ultimate goal for a measurement process would then be both high accuracy and high precision.[5]

There are, of course, other possible sources of error such as systematic and random errors; however, random errors occur in such a manner as to be readily detectable and easily compensated, and systematic errors are usually undetectable.

Examination follows of both the theory and practice of capacitative measurement and the problems involved. The design of the capacitance measurement system considers theory and present experimental results.

B. Capacitance Measurement Considerations

Capacitors

Most capacitors, when examined from a view external to the terminals, i. e., when considered as a black box, can be represented by the three capacitances shown in Figure 11. The direct capacitance C_{HL}, which is the actual capacitance of the unknown, and C_{LG} and C_{HG} the capacitance from the corresponding high and low terminals to the capacitor enclosure surrounding objects and ground.[6] This direct capacitance and the associate ground capacitances are the capacitative values constituting an unknown when the unknown is connected to a measuring device.

There are two modes of measurement for such an unknown: two terminal and three terminal. For two terminal measurement the C terminal is connected
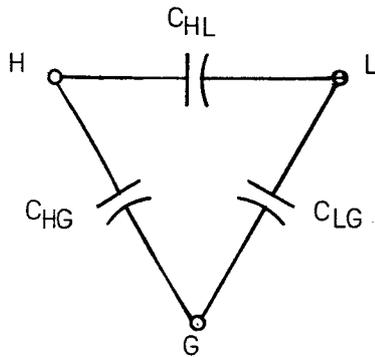
Figure 11
Schematic Diagram of a Capacitor Showing
Direct and Associated Capacitance
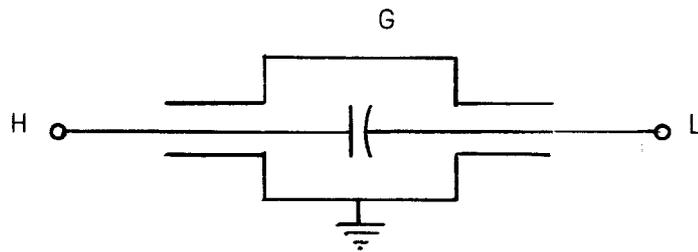
Figure 12
A Three-Terminal Shielded Capacitor
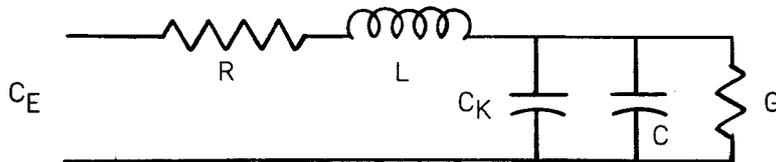
Figure 13
Equivalent Circuit of a Two-Terminal Capacitor

to the case, shorting C_{LG} and the total capacitance is then $C_{HL} + C_{HG}$, where C_{HG} is the capacitance between the high terminal and surrounding objects, and can be changed by changes in the environment surrounding the objects. The most evident factor affecting the environment is the wire connections from the measurement device to the capacitor.

The effect of the surroundings and the resulting uncertainties in measurement they introduce can be eliminated by making three terminal shielded measurements. Figure 12 shows a three terminal capacitor with its associated shield. The capacitances C_{HG} and C_{LG} are eliminated from the measurement circuit by the use of guard circuits which balance the values of C_{HG} and C_{LG} and thus exclude them from the values of direct capacitance (C_{HL}) measured. Thus, it is possible to measure C_{HL} for any capacitor by introducing the desired unknown into a shielded, grounded environment.

Although real capacitors sometimes approach the ideal, there are ⌐ small deviations from ideal performance which must be examined. An equivalent circuit for a capacitor is shown in Figure 13, which shows the lumped constant two terminal form of a capacitor. R is the metallic resistance of the leads, supports and capacitor plates, L the series inductance of the leads and plates, C the actual capacitance of the plates, C_K the capacitance of the supporting structure, and G is the dielectric loss in the supporting insulator, air losses, and ac leakage conductance.

When a non-ideal capacitance is placed in a circuit, two external parameters are of concern. They are the effective value of capacitance at the external terminals and the losses inherent in the device. These quantities are the series reactance and resistance of the device. Figure

-20-

14a shows these schematically. One can also consider the device from a parallel equivalent standpoint. This representation is shown in Figure 14b.

Consideration of total impedance or admittance in the complex plane is shown in Figure 15.where

$$B = \frac{1}{X}, \quad G = \frac{1}{R}, \quad \text{and } Y = \frac{1}{Z} . \tag{18}$$

Also, the power factor for the capacitor is cos θ where θ is the angle between the R and Z or G and Y phasors.

One can define the dissipation factor and storage factor of a capacitor as being ratios of resistance to reactance and susceptance to conductance respectively. In equation form:

$$D \equiv \text{dissipation factor} = \frac{R}{X} = \frac{G}{B} = \frac{1}{Q} = \tan \delta \tag{19}$$

$$Q \equiv \text{storage factor} = \frac{X}{R} = \frac{B}{G} = \frac{1}{D} = \cot \delta \tag{20}$$

where equations (4) and (5) also give interrelations between D and Q.

Thus, it can be seen that the values that are actually measured by whatever system is being used are with respect to the terminals of the unknown.

Two representations for the device, series and parallel are common. The measured values of the unknown can be expressed in either set of parameters, depending only on which is more convenient. We can measure only the resistance and reactive components of the unknown. Figure 15A is the phasor diagram for the series case while the parallel equivalent is represented in Figure 15b.

$$R_s \qquad\qquad X_S = (\omega C_s)^{-1}$$
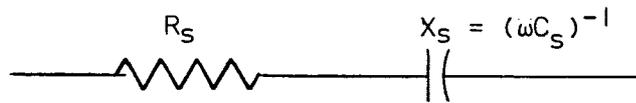
a. Series Representation

$$B_p \;\; = \;\; \omega C_p$$

$$R_p$$
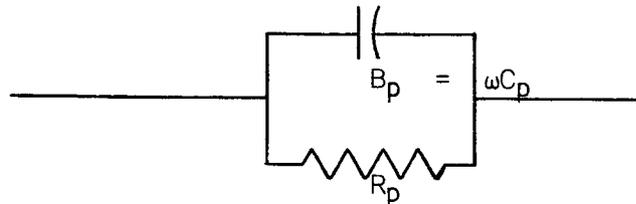
b. Parallel Representation

Figure 14
External Terminal Representation of
a Capacitor as a Circuit Device
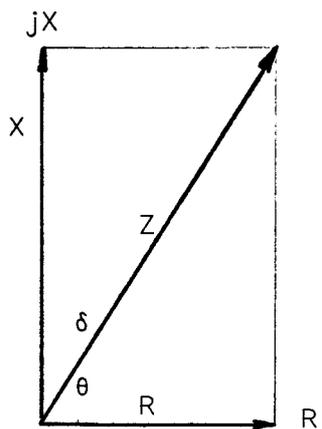
a. Series
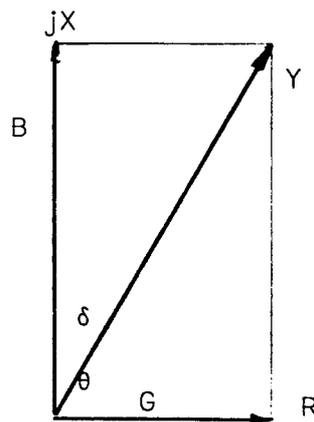
b. Parallel

Figure 15
Imittance of a Capacitor in the Complex Plane

In the series case the dissipation factor D, the cotangent of the dielectric phase angle θ, is

$$D = \cot \theta = \tan \delta = \frac{R_s}{\frac{1}{\omega C_s}} = \omega C_s R_s \qquad (21)$$

where R_s and C_s are the measured values for the series equivalent representation. For the parallel case D is given by

$$D = \cot \theta = \tan \delta = \frac{G}{\omega C_p} = \frac{1}{\omega C_p R_p} \qquad (22)$$

The interrelations between the series and parallel cases are given by:

$$C_p = \frac{C_s}{1 + D^2} = \frac{C_s}{1 + \tan^2 \delta} = C_s \cos^2 \delta \qquad (23)$$

$$R_p = \frac{R_s(1+D^2)}{D^2} = \frac{1 + D^2}{D \omega C_s} \qquad (24)$$

Due to the series inductance, L, of the leads as shown in Figure 13, the terminal capacitance or effective capacitance of the unknown becomes greater than the zero frequency capacitance, C_o. When the frequency, f, is much less than the resonant frequency, f_o, [which is defined by $\omega_o^2 L C_o = 1$] the fractional increase in capacitance ΔC is given by

$$\frac{\Delta C}{C_o} = \omega^2 L C_o = \frac{f}{f_o}^2 \qquad (25)$$

Similarly, the loss D is dependent on frequency, the dependence being:

$$D = \frac{G}{\omega C} + R_1 f \omega C \qquad (26)$$

where R_1 is Resistance at 1 megacycle and f is frequency in megacycles.

This describes a capacitative device as examined from a terminal point of view. When this type of device is connected to a measurement system,

-23-

the parameters measured are the effective capacitance, and the dissipation factor in either series or parallel configurations.

Measurement Devices

High accuracy and precision measurement of capacitative device parameters is generally made by the null method using a variation of the basic ratio bridge. The basic ratio bridge balances for a null or zero dc voltage across a detector by use of either a variable standard capacitor or a fixed standard capacitor and a variable ratio arm. The basic ratio bridge is shown in Figure 16.

After the insertion of C_x, the unknown, in the bridge circuit, C_n, the variable capacitor, is adjusted to obtain a minimum reading on the detector. When this null condition has been established, the bridge is balanced and the value of the capacitor C_N is the value of the unknown. This type of bridge is useable over a wide range of frequency ranges with an accuracy of about 0.01%.

For measurements of greater precision the usual approach is to use an inductively coupled transformer ratio arm bridge. With such a bridge, (Figure 17) accuracies in parts per million can be obtained for ratios as high as 1000:1.

In Figure 17, the primary winding of the transformer (usually toroidal to avoid flux leakage) is used only to excite the core. The voltage in the secondary arms of the bridge is then exactly proportional to the number of turns in the secondary windings. The ratio of the open circuit voltages is equal to the number of turns between taps, and this is easily and precisely determinable. When the number of turns between taps is fixed, the
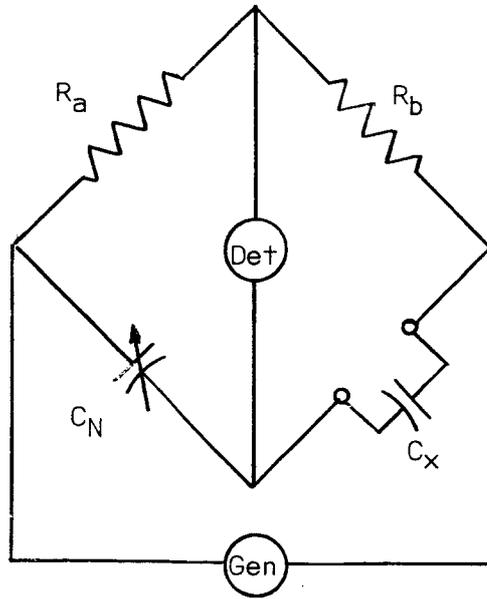
Figure 16
Basic Ratio Bridge
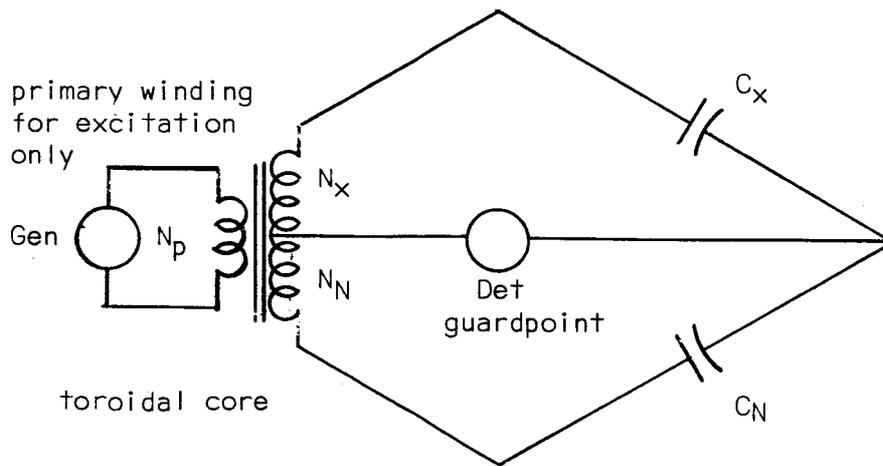
Figure 17
A Simple Representation of a Transformer Ratio Arm Bridge

a. Fixed Ratio –
   Variable Capacitor

b. Multiple Divider –
   Single Fixed
   Capacitor

c. Single Divider –
   Multiple Fixed
   Capacitor
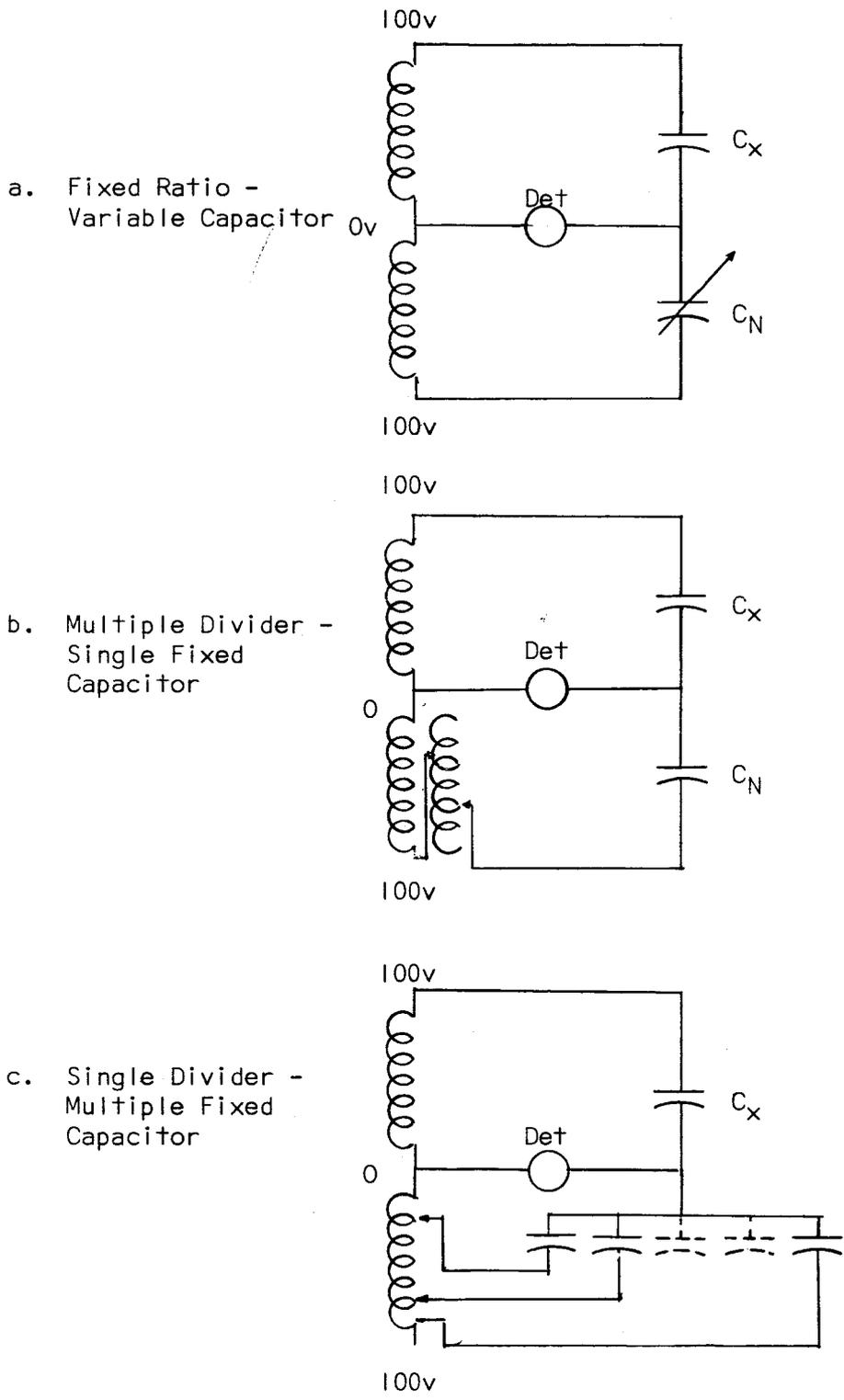
Figure 18
Methods of Balancing a Transformer Arm Bridge

-26-

voltages appearing across these turns is invariant.

The condition for balance, or zero detector current, is then

$$V_N C_N = V_x C_x \text{ or } \frac{C_x}{C_N} = \frac{V}{N_x} = \frac{N_N}{N_x} \qquad (12)$$

With this system, the internal capacitances from the guard point or center tap of the secondary are exactly balanced and do not contribute to the degree of error of the bridge. This bridge measures C_x in terms of C_N without an additional balance. Variations on this general procedure are shown in Figure 18. The three variations shown are:

  1. Fixed ratio - variable capacitor

  2. Multiple divider - single fixed capacitor

  3. Single divider - multiple fixed capacitor

The General Radio Model 1615A Transformer Arm Ratio Bridge

Figure 19 shows a simplified circuit of the General Radio Model 1615A capacitance bridge. As can be seen from Figure 19, the General Radio Model 1615A uses a single decade of transformer voltage division and multiple fixed standard capacitors to provide six decades of resolution of capacitance. Through use of the variable resistances G and D four decades of loss or conductance are obtainable. There are eight standard capacitors, of which only six may be used at any one time to give six figure resolution for capacitance values. There are four precision decade resistors connected in series to give foursignificant figures for D and four precision decade resistors connected in parallel to give four significant figures for G.

On this bridge either C_p and G may be measured on C_s and D, depending on how "lossy" the device being measured happens to be. The choice is G for

more lossy devices.

Other features of the General Radio 1615A Bridge are:

1. Two or three terminal measurement.

2. Use of external standards to extend D and/or G ranges.

3. Use of external standards for measuring difference between the unknown and the external standard.

4. Wide frequency range.

5. Easily adopted to use with external power supply for dc bias of unknown being measured.

6. The General Radio 1615A Capacitance Bridge is furnished in the General Radio Model 1620A Capacitance Measurement System with the appropriate oscillator and detector, i. e., the system is furnished complete as the General Radio Model 1620A Capacitance Measurement System.

Comparison of the General Radio Model 1620A Capacitance Measurement System with Other Available Bridges and Reasons for Selection

On the basis of manufacturers' literature, three capacitance measurement bridges were chosen for more critical evaluation. These were: the General Radio Model 1615A, the Electro-scientific Industries Model 277, and the Wayne Kerr Model B221A. At first examination, all of these bridges appeared to meet the requirement for the project capacitance measurement system.

The Wayne Kerr Bridge is a transformer ratio arm bridge suitable for two, three, or four terminal measurement, and is capable of making measurements in any quadrant of the complex plane. This bridge makes use of two precision transformers - one for signal input and the other to the detector. The

6 decades of C
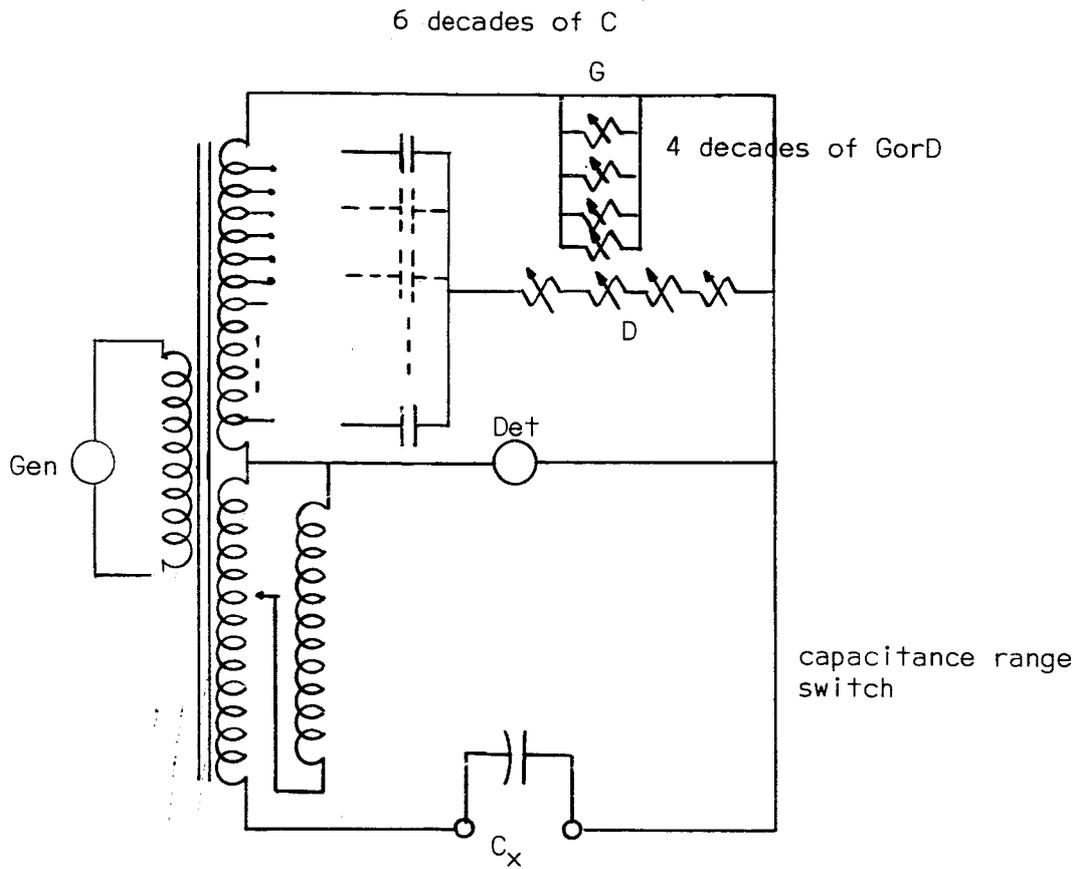
Figure 19
Simplified Circuit Diagram of the General Radio
Model 1615A Transformer Arm Ratio Bridge
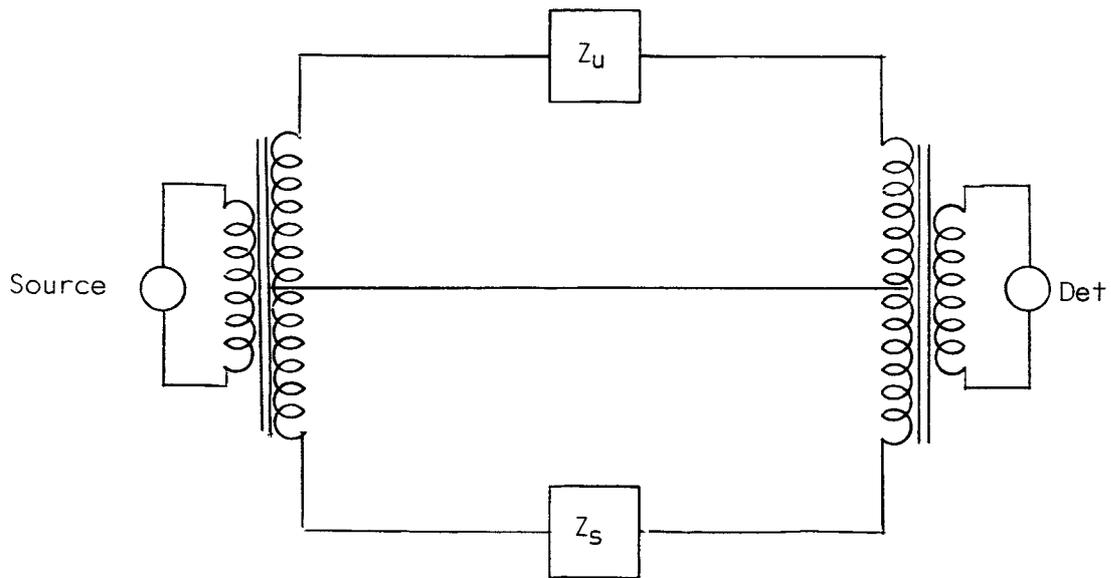
Figure 20
Simplified Circuit Diagram of Wayne Kerr Model

bridge balances the unknown Z_u against a standard Z_s. The use of two transformers gives a comparison range of 10^6 to 1. (Figure 20)

The manufacturer specifies four significant figures with an accuracy of the order of 1% or greater. It was felt that this bridge would not produce measurements of the required accuracy, and it was not given further consideration.

The General Radio Model 1615A and the Electro-scientific Industries Model 277, with the recommended oscillators and detectors, were evaluated in the laboratory. The Electro-scientific Industries Model 277 bridge is a revision of the basic ratio-arm bridge as shown in Figure 21.

Unknown capacitance with its associated lloss tangent is inserted in the unknown terminals and the bridge is balanced by a series of standard capacitors shown as C_{var} in Figure 21.
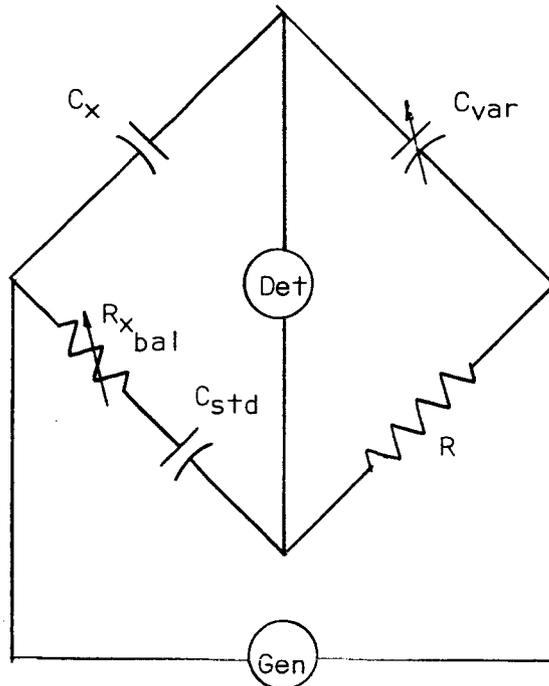
Figure 2I
Simplified Electro-scientific Industries
Model 277 Capacitance Bridge

Data Produced by the Capacitance Measurement System

To check the operation of the bridge system, a p-n junction diode capable of withstanding a reverse bias of the order of several hundred volts was placed in the sample holder. A series of capacitance measurements were made. The log-log plot of the bias voltage applied in the reverse direction versus the value of capacitance measured is shown in Figure 25 . As can be seen from the plot the slope is approximately -I/3. This implies that the p-n junction measured is of the graded junction variety. For a graded junction the expression for capacitance is:

$$C = \left[\frac{qa\epsilon^2}{12|v|}\right]^{1/3} = k \left[|v|\right]^{-1/3}$$

After thorough comparison of these bridges, the General Radio Model 1615A Capacitance Bridge Measurement System was selected for use for the reasons listed below:

1. The General Radio Bridge allows measurement of capacitance to a greater number of significant figures.

2. The General Radio Bridge has a definite advantage over the Electro-scientific Industries model in regard to the method of application of bias, i. e., it requires very little in the way of an external bias circuit.

3. The General Radio Bridge has greater degree of accuracy since the accuracy in the Electro-scientific Industries bridge is in terms of $\pm$ 1 dial division, and the General Radio bridge is in terms of the value of the unknown.

4. The General Radio Bridge has a better system of three terminal measurement with the use of shielded cables that cancel the terminal to ground capacitances.

5. The measurement of D, the "dissipation factor" on the Electro-scientific Industries bridge is less accurate than on the General Radio bridge, i. e., it has a very broad null.

6. The digital readout of the General Radio bridge is much easier to read than the Electro-scientific Industries bridge.

7. The General Radio bridge system is more difficult to obtain an initial balance, but the successive "difference" measurements are easier.

8. Frequency selection is much greater in the General Radio system.

Project Capacitance Measurement System

Figure 22 shows a block diagram of the system presently in use.
The 1615A Capacitance Bridge is, of course, the central piece of equipment.
The ac signal for measurement is supplied by a General Radio Model 1210C
oscillator to cover a frequency range of 20 cps to 100 kc. The oscillator
is powered by a General Radio Model 1203B unit power supply. For our purposes
the output range is zero to seven volts with sinusoidal waveform.

The dc bias is supplied by Kepco 0-30 Model ABC power supply and a
Kepco Model B 0-400 volt power supply for the higher voltage ranges. Both
of these power supplies are continuously variable over their entire ranges.

The General Radio Model 1232A tuned amplifier and null detector is
used with the bridge. After the maximum bridge setting below the noise
range is obtained on the gain of this instrument, the output is monitored
by a Hewlett-Packard 425A VTVM dc microvolt ammeter. For extremely sensitive
balances this output is monitored by a Keithley Model 149 dc milli-microvolt-
meter.

Due to the identical nature of the terminals for shielded measure-
ment and unshielded three terminal measurement on action of the measurement
switch, the ac and dc voltage levels appearing across the sample are monitored
by Hewlett-Packard 400H VTVM and Hewlett-Packard 413A DCVMS respectively.
The switch is then returned to the shielded position for measurement.

C.   Laboratory Measurements

It is a long step from the theory of capacitance measurement to the
production of satisfactory experimental data. The problems encountered in
attempting to produce data are of assorted variety and different natures.

-33-
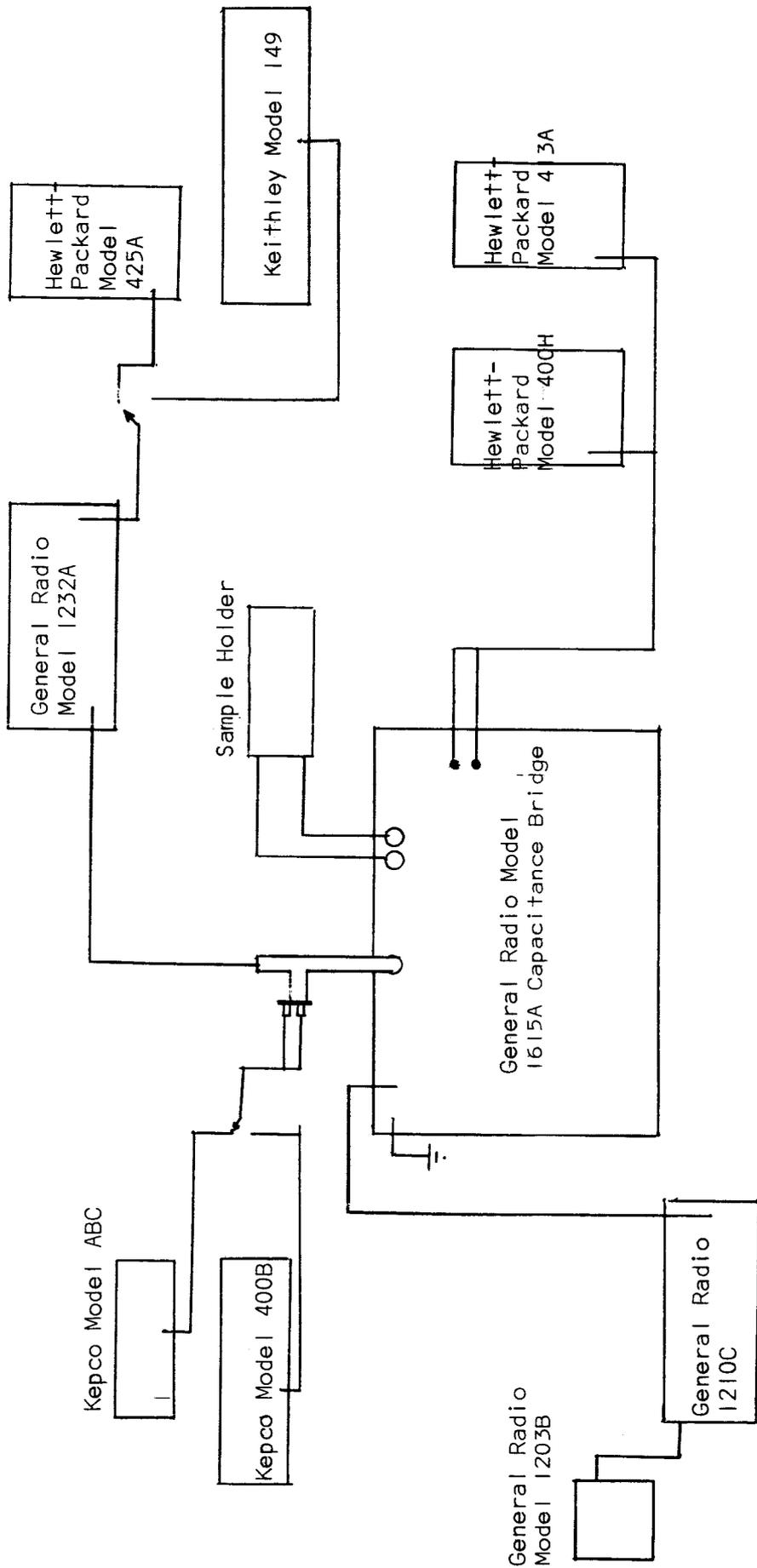
Figure 22
Capacitance Measurement System

In state-of-the-art measurements such as are being attempted, some factors have to be considered that might ordinarily be ignored. Three terminal shielded measurement of capacitance was selected as mode of measurement for our project due to the isolation from surrounding stray signals produced by the shield around the device.

Some of the problems encountered during the process of setting up and checking out the capacitance measurement system are discussed below, and the present solutions to the problems are given.

Sixty Cycle Hum

One of the ever present problems of electronics measurement and design is the 60 cps ac voltage induced in circuits due to the presence of 117 volt 60 cps power provided as the normal power supply in all buildings. Although the magnitude of this induced voltage is not large, and can normally be neglected, due to the magnitude of the signal level we use in measurement (on the order of several millivolts), the magnitude of the 60 cps "hum" becomes significant. This problem was minimized by moving the entire capacitance measurement system to a screen room having 120 db attenuation at 400 mc and taking great care in the arrangement of component units of the system and in the grounding of the system. As a further precaution, all leads interconnecting the portions of the system specifically necessary for measurement have been shielded. Also, all ground loops have been avoided, as far as is known. The only 60 cps signal present in the screen rooms is the supply for the instruments. As this is a regulated supply there are almost no stray fields, since the input is 3 wire, single phase, 117 volts. The lights in the screen room are 12 volt dc to eliminate any other source

-35-

of ac voltages.

DC Bias

To provide the dc bias voltage for our samples, the dc power supply was connected as shown in Figure 22. Although the application of dc bias was simple enough, a method for the measurement of the actual value of dc bias existing across the sample was not readily apparent. It was found that the identical dc bias potential across the shielded terminals appears across the unshielded three terminal binding posts. Thus, a dc voltmeter may be connected across the three terminal binding posts and by use of the selector switch between types of measurement the existing dc bias may be measured without loading the voltage across the probes in the sample holder. This means that once the sample is inserted in the sample holder the conditions of bias existing across the sample may be determined by using the selector switch. DC bias will be measured to approximately four significant figures.

AC Signal Levels

It was thought at first that signal level could be set and measurements carried out for capacitance. Due to the nature of the bridge used, however, signal level must be varied to obtain the best balance. The procedure used will be to balance the bridge using variation of the signal level and then while attempting to hold the balance to minimize the applied ac signal level. It is believed at this time that the minimum signal level that can be obtained and consistently held will be of the order of several millivolts.

Circuit Parameters

As was seen in Figure 13, the equivalent circuit of a two terminal

physical capacitor has associated parameters to account for the non-ideal behavior of the device. At this point in the program and due to the comparative magnitudes of these parameters, these parameters R, L, and C_K shall be neglected. R, the resistance of the leads, is of the magnitude of one ohm and is much less than the sample resistance. C_K, the capacitance of the mounting and all associated, is neglected due to the nature of shielded three terminal measurements. The capacitance of the leads and mounting is balanced out by appearing on both sides of the unknown. The inductance of the leads is neglected as a second order effect at this time.

Sample Holders

The use of three terminal measurements requires some type of sample holder and associated shield. The requirements of this device are simple. First, it must provide shielding from environmental electrostatic fields; second, it must provide a mounting for the sample; third, it must provide electrical connections for signal and bias. Figure 23 shows a schematic of the sample holder presently in use.

This is a relatively simple sample holder, and Figure 24 shows a tentative revised version that is in the process of being designed. The second version (Figure 24) is to be capable of being used at low temperatures.
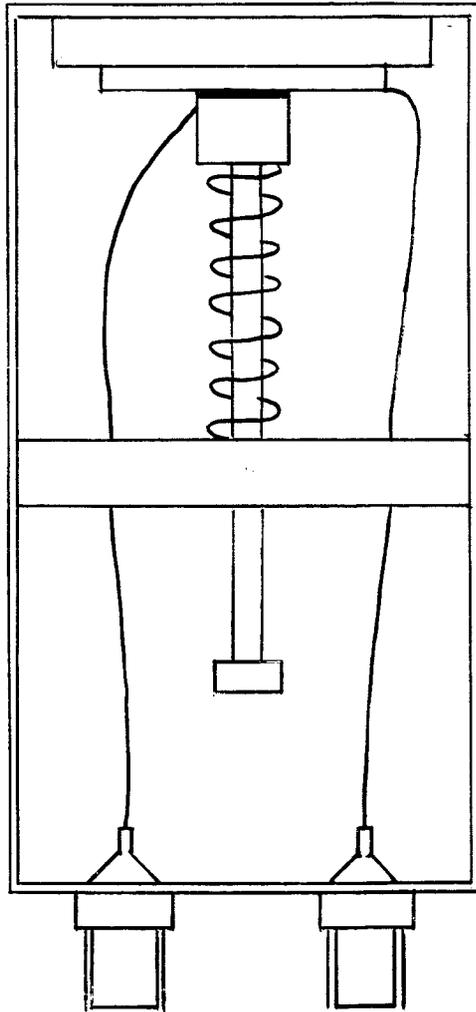
Figure 23
Sample Holder for M-O-S Diodes
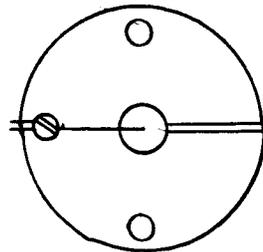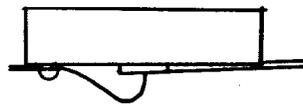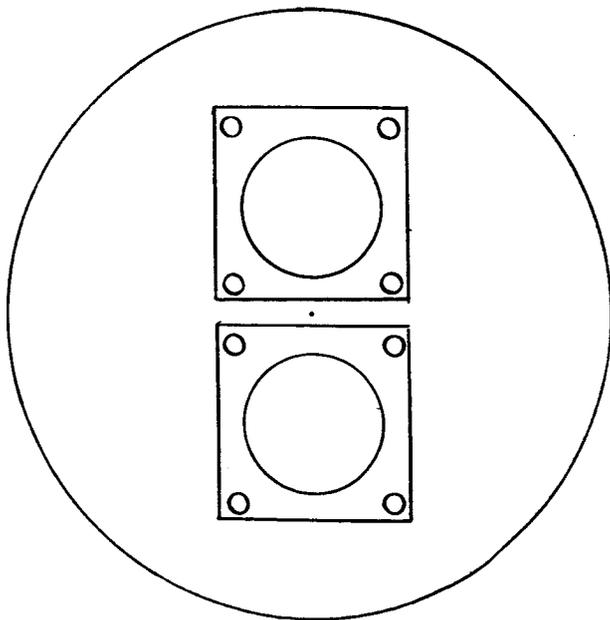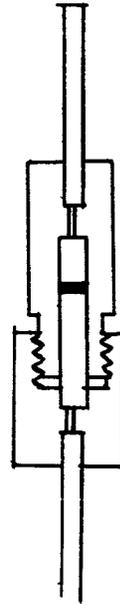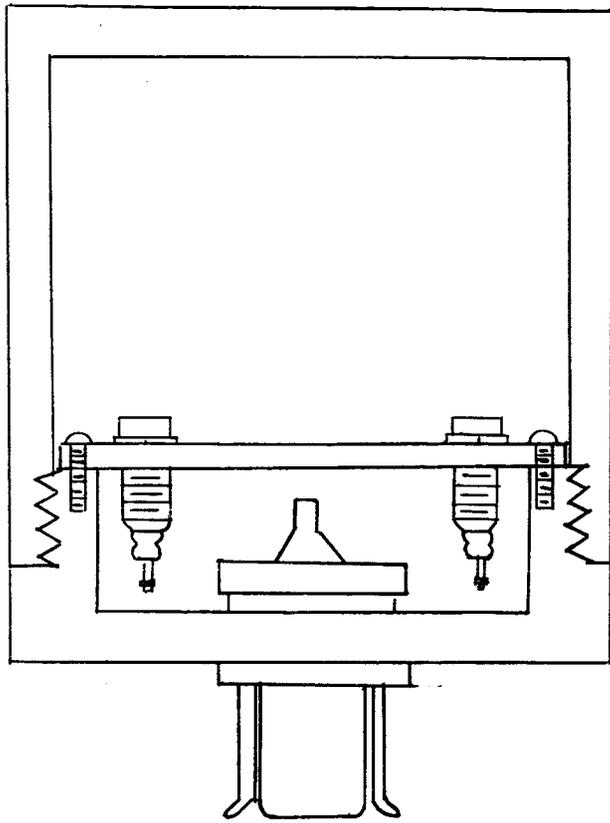
Figure 24
Revised Sample Holder
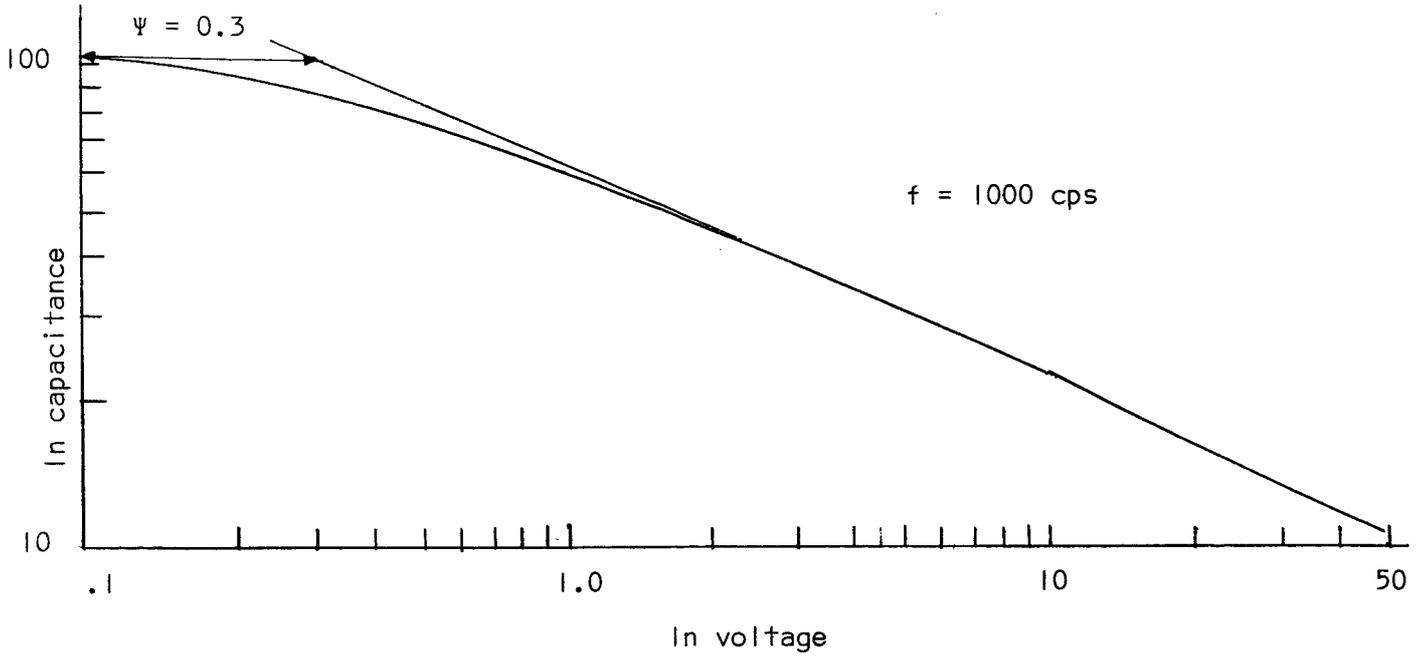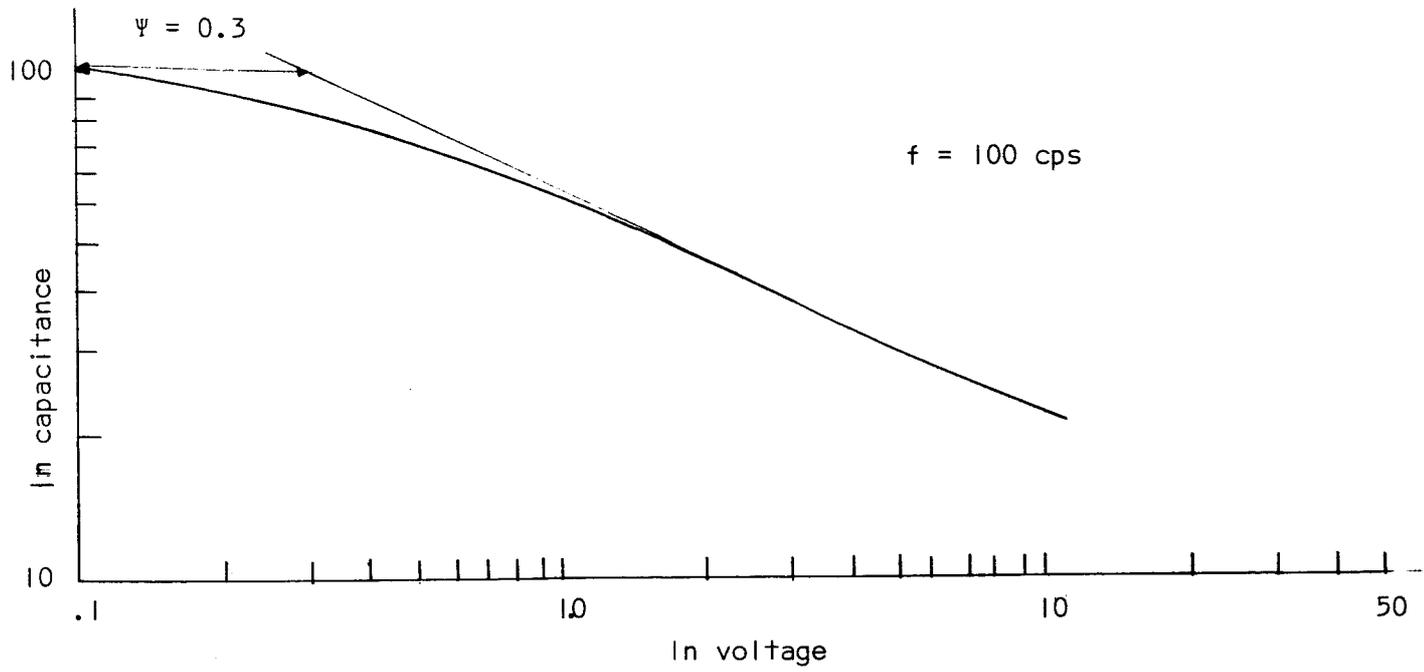
Figure 25a and 25b
Capacitance Versus Voltage of a P-N Junction
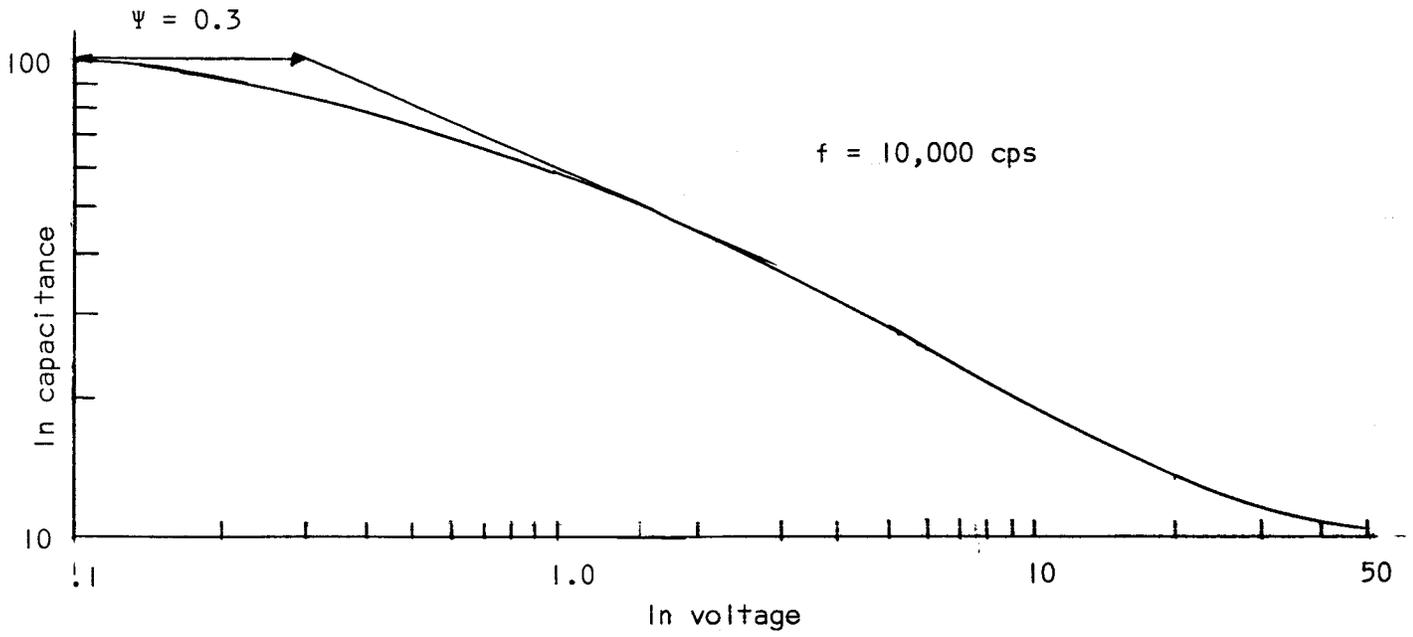
Figure 25c
Capacitance Versus Voltage of a P-N Junction

Measurements were made at three frequencies: 100 cps, 1000 cps, and 10,000 cps.

It should be noted that as the values of capacitance measured become smaller the nulls become harder to obtain. At a frequency of 100 cps, it was not possible to obtain a null for bias voltages greater than 10 volts. These measurements indicate the need for the development of experimental techniques for the measurement of small values of capacitance.

Tables 1, 2, and 3 in the appendix give the specific values of voltage applied and capacitance measured.

Review and Discussion

In the preceding sections of this report we have discussed the nature of charge storage devices and the theory of equipment to measure the external parameters of these devices or capacitors. The advantages and disadvantages of several applicable capacitance measurement systems have been presented and the system selected for use has been described. Additional techniques of capacitance measurement for the production of accurate, useful data are being developed to supplement basic known techniques.

There are certain problems that need to be solved before complete confidence may be had in the capacitance-voltage data throughout the entire range of measurements. For values of capacitance, say around 1000 pf and greater, a good six significant figure value of capacitance may be obtained. However, as the value of capacitance becomes smaller the many significant figure balances become harder to obtain since a comparatively good null can be established for small capacitance with only three or at the most four significant figures. Thus, there is a problem of measuring devices with

high leakage current. The bridge does not balance sharply for capacitance values of the order of one hundred picofarads and less.

When measuring small values of capacitance, a null balance is difficult to obtain. After the first three significant figures are obtained, the balance, or null, condition is well established, and the production of successive significant figures calls for the utmost in sensitivity. An alternative method of producing data is possible with the General Radio Model 1615A bridge. It is possible to balance this bridge to read the difference between an external standard and the unknown. Judicious selection of the external standard would place the difference measurement in the range where a balance condition is reflected in five or six significant figures. Mathematical correction can then be made to produce experimental data on the unknown.

When the device producing the capacitance being measured has a dc leakage current caused by applied bias corresponding to values of loss tangent of the order of 0.40, the bridge cannot achieve a meaningful balance. This situation may be improved by measuring the parallel capacitance and conductance of the device, but conductance is limited to values less than 0.1 micromhos. If the loss of the device exceeds these values, a direct balance cannot be obtained. In these cases, the physical structure of the device might better be understood if data could be obtained and comparison made to a device with normal loss.

A possible method for obtaining this data would be to connect a capacitor with very low loss and large capacitance in parallel with the unknown. This would effectively increase the capacitance seen by the

bridge while decreasing the loss. This allows a balance to be obtained, and mathematical manipulation of data would give the capacitance and loss or conductance of the unknown.

These techniques, when fully developed, will expedite the generation of capacitance-voltage data. They will allow the examination of devices with wide lattitude in parameters and contribute to the formation of the theory describing the physical processes that act in the device.

IV. Electron Microscopy

A. Etching Technique

To complement the information obtained from the capacitance and voltage measurements, a simultaneous study of the interior structure of silicon is being made using the techniques of transmission electron microscopy. The primary problem in this study at this time is producing samples which are thin enough to transmit an electron beam. To yield useful information, the transmitted beam must have enough intensity to produce a recognizable image. Sufficient intensity is usually obtained if the samples are less than a 1000 Å thick; ideally the sample should be less than 500 Å thick. The electron microscope to be used in this study and the general procedure and apparatus which will be used to produce samples suitable for use in the electron microscope were discussed in the last report. In this section of this report a brief summary of the theory of electrolytic etching of silicon will be presented first. Next, the results of our efforts to date and the problems encountered will be presented.

Electrolytic Etching of Silicon

Electrolytic etching or electropolishing is often defined as the uniform removal of surface atoms with an atomicly smooth surface as the desired end result. The most successful work reported in the literature has been accomplished using aqueous solutions of hydrofluoric acid, HF. Some work using strong alkaline solutions has been reported but these solutions chemically attack the silicon resulting in preferential etching and rough surfaces. Some fluoride salts are satisfactory for etching; however, the salts used and the final product of the anode reaction when

using these salts must be soluble in water. HF and its anode product hydrofluosillicate, H_2SiF_6, are highly soluble in water and it is for this reason that aqueous solutions of HF have been preferred for electrolytic etching of silicon.

It has been proposed that electropolishing of silicon begins when the HF begins to be used as fast as it arrives at the surface being etched. When this condition is met, a thin film, which is suggested to be SiO_2, is present on the surface. The exact dissolution process that occurs at the silicon surface is not known; however, the following process has been proposed. Each atom of a single crystal of silicon is covalently bonded to two underlying silicon atoms. When these bonds are broken by the arrival of a hole for each two-electron bond, the silicon atom combines with available oxide or hydroxide ions. The process may be as follows:

$$Si + 2H_2O + z e^+ \longrightarrow SiO_2 + 4H^+ + (4-z)e^-$$
$$\big\downarrow 6HF$$
$$\longrightarrow H_2SiF_6 + 2H_2O$$
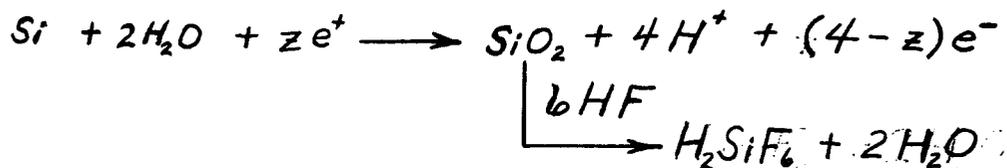
When the HF is not consumed as fast as it arrives at the silicon surface, a more complex reaction occurs resulting in the formation of a thick film on the surface. Films grown in electrolytes with a high concentration of HF ($\sim 50\%$ HF) have been found to be almost all silicon. The following chemical process has been proposed.

$$Si + 2HF + ze^+ \longrightarrow SiF_2 + 2H^+ + (2-z)e^-$$

$$\text{rapid} \quad \longrightarrow Si + SiF_4\uparrow$$

$$\xrightarrow{2HF} H_2SiF_6$$

$$\text{slow} \quad \xrightarrow{H_2O} SiO_2 + 2H_2\uparrow$$

$$\text{rapid} \quad \xrightarrow{6HF} H_2SiF_6 + 2H_2O$$
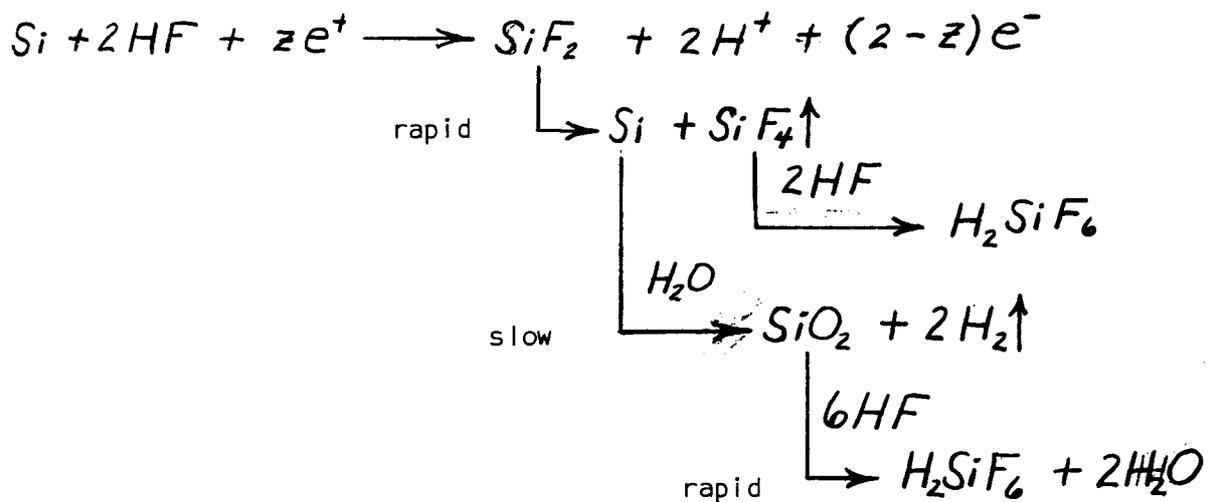
The slow reaction of the Si and water is the reason for the build up of the silicon film on the anode surface.[9]

As mentioned above, holes are essential to the dissolution process. In p-type silicon holes are the majority carriers and consequently they are readily available. In n-type silicon, however, holes are the minority carriers and because of their short supply, some method must be used to generate and make them available at the silicon electrolyte interface if the etching process is to proceed at a reasonable rate. The easiest way to produce these holes is by high-intensity illumination of the working surface with light of wavelengths shorter than 1.2 microns. Those wavelengths longer than 1.2 microns only add heat to the sample and should be filtered out if possible.

Experimental Results

To date we have been able to produce several samples in which small areas were thin enough to be used in the electron microscope. Starting with

a silicon die 1/8" in diameter and about 0.030 inches thick, we can obtain
a semicircular area with a thickness of less than 500 Å thick. The total
usable area in these samples has been about one-tenth of a square milli-
meter. We seek to obtain an area one millimeter in diameter with a uniform
thickness of approximately 500 Å. The major part of our efforts during the
period covered by this report have been directed toward achieving this
result. The problems encountered can be separated into three interrelated
areas: (1) jet electrode position characteristics, (2) electrolyte com-
position, and (3) etching characteristics of the bulk and thin sections of
the sample. This separation is arbitrary and only for the purpose of dis-
cussion. The discussion of the problems begins with a brief summary of the
procedure used to obtain the thin samples.

Jet Electrode Position Characteristics: The current density, which
will be discussed later under etching characteristics, is highly dependent
upon the position of the jet electrode in relation to the working surface
of the sample. Increasing the distance between the jet and surface by one
millimeter can sometimes reduce the current by a factor of two or more.
The electrolyte composition determines the magnitude of current change
with distance of the electrode. It is desirable to have a high current
density; therefore, in the samples produced to date the jet has been
positioned about one mm from the surface of the sample as the desired
thickness is approached. Having the jet this close to the surface intro-
duces another problem, however. In this position the current density is
not uniform throughout the electrolyte. The resistance of the electrolyte
is such that the portion of the sample closest to the jet is subjected to

a higher current density. Because of this a circular ring on the sample surface is etched at a higher rate, thereby producing a thin section of non-uniform thickness. Although the thin section is small and non-uniform, the current density in this area is apparently uniform because preferential etching is not apparent when the sample is observed in the electron microscope.

Electrolyte Composition: The electrolyte used so far has been composed of isopropyl alcohol, water and hydrofluoric acid. The composition of the electrolyte is critical for two primary reasons. With high concentrations of HF, a brown deposit is formed on the surface of the sample. The amount of deposit is a function of both the current density and HF concentration. For a given amount of deposit, the required current density increases as the HF concentration decreases. It is felt that this deposit is the same as that described during the discussion on the theory of etching. When the HF concentration is too low, non-uniform etching occurs. The sample will have a polished surface, but when the sample is examined with an optical microscope small dimples or impressions can be seen. In addition to the uneven surface, a considerable amount of time is required for the etching process.

Etch Characteristics of Bulk and Thin Sections: In general, it appears that the surface condition is essentially a function of the current density for a given electrolyte composition. At low current densities small pits appear on the etched surface of the sample. Usually, these pits are large enough to be seen clearly with a 30 power optical microscope. However, at times they are so small and closely spaced that the sample surface appears to have been sand blasted, even when observed with a microscope.

As the current is increased these pits disappear and the etched surface takes on a mirror-like finish. When the current is increased still further, the brown film previously discussed appears on the surface and the amount of film increases with the current.

The conditions described above apply to etching of the bulk sample where the resistance of the sample is uniform over the surface being etched. If the surface being etched is thin (< 5000 $\overset{o}{A}$) the condition of uniform resistance of the thin section no longer holds. The resistance of the thin section increases as the thickness decreases. As a result, the current density in the thin section, which is the area of primary interest, decreases leading to preferential etching and the formation of etch pits. It is felt that these etch pits can be eliminated or at least reduced if additional fluoride ions are available from a modified solution composition.

Summary of the Results: The best samples that have been produced so far have been etched using an electrolyte volume composition of 85 parts alcohol and 15 parts 48% HF. The current used has been about 40 ma with the jet electrode about 1 to 2 mm from the working surface. As mentioned earlier, the samples produced have had very small areas which are useable in the electron microscope. As an indication of our efforts to date, some photographs are presented on the following page. A complete interpretation of what can be seen in these photos is not available at this time.

Both photographs are from the same sample but different areas. There are three points of particular interest. The broad dark lines appear to be lines of constant sample thickness as they appear to move when the angle of incidence of the electron beam is charged. The narrow lines in the top
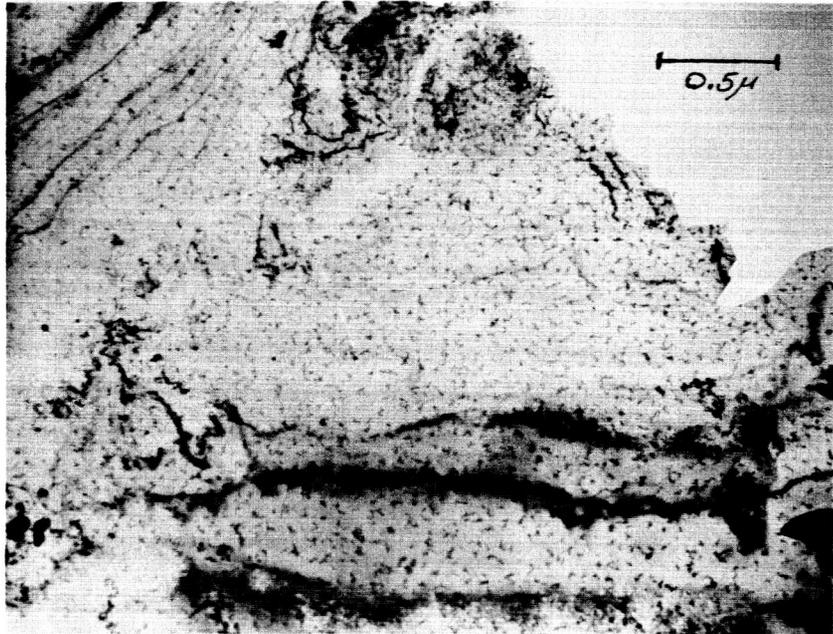
Thin Section of 30 ohm-cm., p-type Silicon (32,000X)

Figure 26a
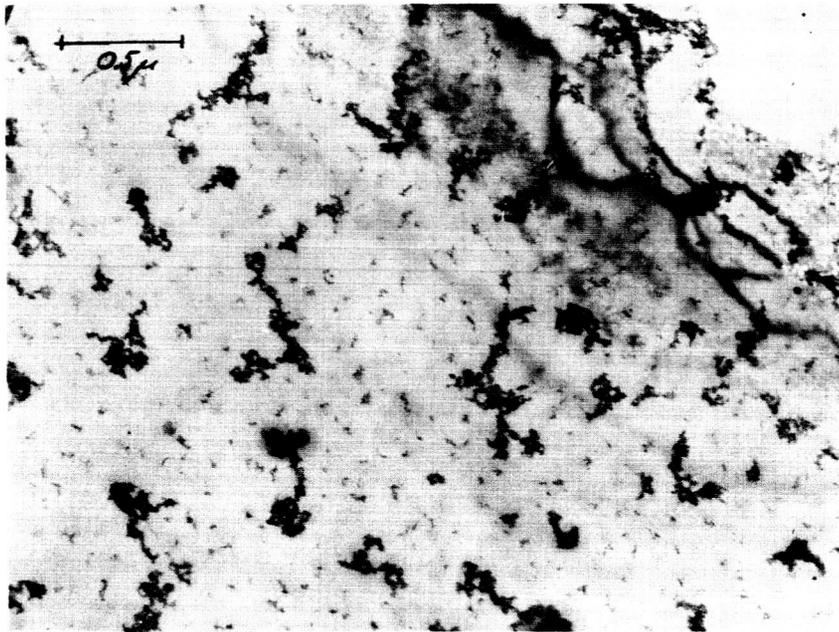
Thin Section of 30 ohm-cm., p-type Silicon (32,000X)

Figure 26b

portion of the top photograph do not move when the angle of incidence is changed but instead they go in and out of contrast and for this reason they are assumed to be dislocations. The spots that appear in both photographs are believed to be segregated impurities. From the point of view of etching results, the area covered by each photograph is comparatively uniform in thickness. We have demonstrated how to produce thin samples suitable for transmission electron microscopy. The problem, as it stands now, is producing samples with larger areas of thin sections consistently and interpreting the structure observed in the electron microscope.

B. Replication Techniques

A replica is a cast of a specimen which is opaque to electrons and permits their surface structure to be studied in the electron microscope. The replica consists of a thin film of electron-transparent material corresponding exactly to the surface topography of the specimen. By using this film one will be able to study irregularities in the silicon surface, the SiO_2 layer, and the $Si-SiO_2$ interface. A discussion of the Formvar/carbon replicating process was given in the August 31, 1964 Quarterly Report and will not be repeated here. Instead, other methods which have been tried will be discussed concerning problems encountered and results obtained. All of the methods tried have been two-step processes of one form or another since the single-step process (applying the carbon film directly to the surface of interest and then stripping or separating the film from the surface of interest) has the inherent disadvantage that the surface being investigated must be dissolved away and destroyed during the stripping process. The two-step process involves making a preliminary impression on the specimen surface in one material, coating the structure surface of this impression with the final replicating material, separating the two, and examining the replica in the electron microscope. This preserves the specimen for further use. The replicas made in the laboratory so far have been replicas of a thin slice of silicon cut on the diamond saw.

Replicating Tape Method

A replica can be made by using a type of plastic "Replication Tape" sold by Ladd Research Industries, Inc. Either side of the "Replication Tape" may be used. The replica is made by placing a drop of acetone on the surface

to be replicated then immediately placing a small square of plastic on
the acetone. The acetone softens the plastic which then follows the con-
tour of the specimen surface thus making a faithful replica of the surface.
Little or no pressure is necessary at this stage. The replica is ready to
be stripped from the specimen surface when the plastic is dry. This
usually takes about five minutes. The plastic replica formed is mounted,
replica side up, on a glass microscope slide. "Scotch Tape" can be used
to hold the plastic replica in place. A coat of carbon is then vaporized
onto the replica side of the plastic tape. The actual carbon evaporation
will be discussed later. At this point one of two things may be done.

(1) The route taken in this laboratory is as follows: At this
point shadow the replica with a coat of platinum or platinum-carbon.
Shadow casting is a technique which will be discussed later. The plastic-
carbon replica is now removed from the vacuum chamber, and the plastic is
ready to be dissolved away. This is done by placing the carbon-plastic
replica in a small petri dish partially filled with acetone. The acetone
dissolves the "Replicating Tape" and the carbon film floats free. The pro-
blem encountered so far has been the fact that the carbon film tends to
come to pieces and breaks apart as it floats off of the tape. A piece of
the carbon film large enough to study in the electron microscope can usually
be "caught" on a microscope grid, but it is feared that later when interest
lies only in a very specific area of the specimen that difficulty might be
encountered in "catching" the right part of the film. The carbon replica
obtained in this manner showed a good replica in the electron microscope.
This is shown in the accompanying photograph.
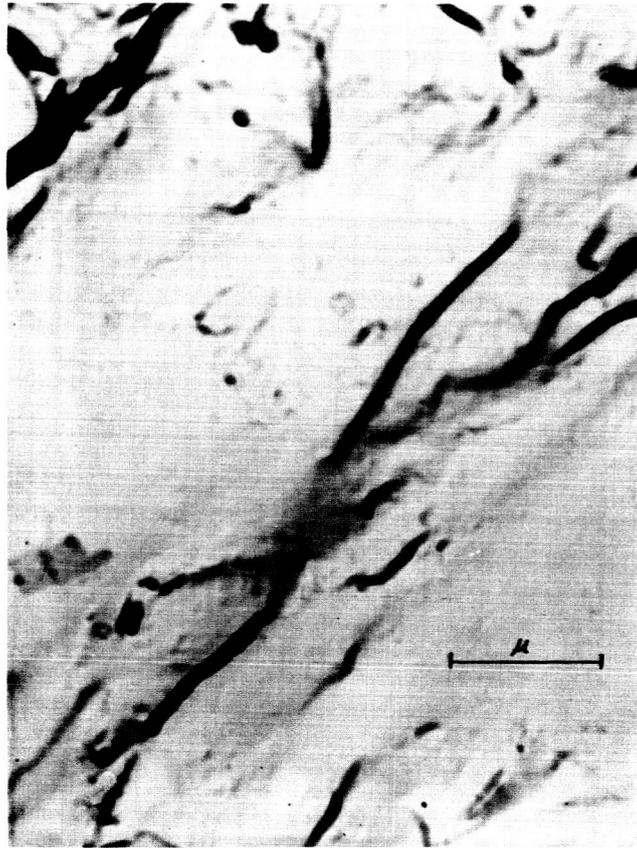
Figure 27

Replica of Silicon Sliced on Diamond Saw

Carbon Replica - Platinum Shadowing

Negative 10,000, Photo Enlargement 1.5X

The replica in Figure 27 was made in the manner previously described.
The dark lines running diagonally across the photograph are 3μ apart. From
the rotary speed of the diamond saw blade and the transverse speed of the
blade, these lines can be justified as saw marks since one point on the edge
of the blade cuts the specimen every time the specimen moves approximately
three microns. The dark places are deposits of platinum from the shadowing
process. Thus if one looked at a cross sectional view of the specimen from
the direction of the arrow, a topography similar to Figure 28 would be observed.
It must be kept in mind that this method produces a negative of the original
surface.
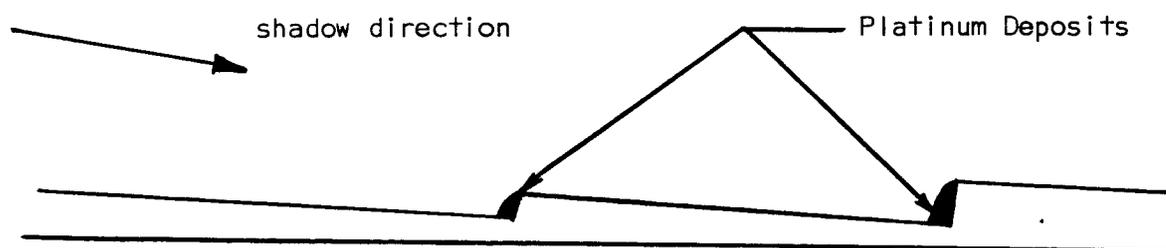
Figure 28
The Silicon Surface

The other irregularities in the photograph are simply surface ir-
regularities and imperfections on the silicon surface.

(2) An alternative route which may be taken after the coat of
carbon is vaporized onto the tape is as follows: Remove the plastic-carbon
replica from the vacuum chamber and then spread a thin (about 2mm) film of
dental wax over the carbon side of the replica. This can be done by melting
the wax in a small beaker and then spreading the wax over the replica with
a warm glass rod. Dissolve the plastic part of the replica from the carbon-

wax part of the replica by placing the complete-replica-(plastic-carbon-wax)
into a small petri dish partially filled with acetone. For ease of manipula-
tion, place the wax side down so that it rests against the bottom of the petri
dish. Use several changes of acetone over a period of several hours. All
debris must be removed before proceeding to the next step. Now mount the
carbon-wax replica on a glass microscope slide using Scotch Tape as described
previously. The carbon side must face up and care should be taken so that
the wax side of the replica does not stick very tight to the scotch tape.
If the wax sticks too tight to the tape, it will be difficult to remove it
from the tape without damaging the replica. Place the mounted carbon-wax
replica into the vacuum coating unit and shadow lightly with platinum-carbon.
This will be discussed later under "Shadow Casting." Remove the shadowed
carbon-wax replica from the vacuum chamber and scribe the carbon part of
the replica into small squares about 1/8" square. Alternatively, the complete
carbon-wax replica can be cut into small squares. Place the scribed or cut
replicas in a small petri dish containing xylene. The xylene will dissolve
the wax and the carbon part of the replica will float free in the xylene.
Transfer the carbon replicas through several changes of xylene or until the
carbon replicas are clean. Slight heat will accelerate this procedure con-
siderably. Now pick up the clean carbon replicas from the xylene solution
with clean copper specimen grids and drain off excess xylene with filter
paper. If the replicas are not yet thoroughly clean, then try an additional
rinse with ethylene dichloride. This method has the advantage that perhaps
the carbon would hold together better with the aid of the wax and also this
method produces a replica of exactly the same shape as the specimen surface

whereas the first alternative produced a negative of the original surface (hills appear as valleys, valleys appear as hills).

Collodion Method

Another method of interest is the collodion method. This method is similar to the Formvar/carbon method described in the August 31, 1964 Quarterly Report, but it has enough differences to merit its discussion here. This method was first tried in the laboratory as follows: Place a drop of collodion on the sample, drain off the excess and let dry for about five minutes. Now place a piece of Scotch Tape over the collodion, press down, and carefully pull off the tape being sure that the collodion strips off with the tape. Now place the collodion replica and Scotch Tape in the evaporator and evaporate carbon onto the collodion. Next shadow with platinum or platinum-carbon. Take the tape-collodion-carbon out of the vacuum and dissolve off the Scotch Tape with ethylene dichloride. The collodion-carbon replica is then placed in a small petri dish partially filled with amyl acetate to dissolve the collodion and allow the replica to float free. The same difficulty was encountered here that was encountered with the "Replicating Tape" method, that is, the carbon seems to split apart as it floats free and, although it is easy to catch some piece of carbon, it is difficult to catch a particular piece. However, pieces of carbon have been caught on grids from this method and proved to be good replicas for study in the electron microscope.

In seeking to overcome this difficulty, the following method was used: Put a drop of collodion on the sample and let dry. Place a microscope grid on the collodion which is on the specimen. Put another drop of collodion

-58-

on the grid to hold the grid in place. Now place the Scotch Tape on the combination, carefully strip off, and proceed as before. It was felt that the grid being under the carbon would help contain the carbon and prevent it from shredding apart quite so much. However, this was not the case and nearly as much difficulty was encountered as before.

The following alteration was devised to contain the carbon replica on the electron microscope grid. The above method is used to the point where one is left with carbon-collodion-grid-collodion-Scotch Tape. At this point the tape is dissolved off with ethylene dichloride and one is left with carbon-collodion-grid-collodion. This combination is then placed in a jig as shown in Figure 29. By heating the amyl acetate and passing vapors over the replica the collodion will be dissolved away and one will be left with the carbon replica on the grid ready for examination in the electron microscope.
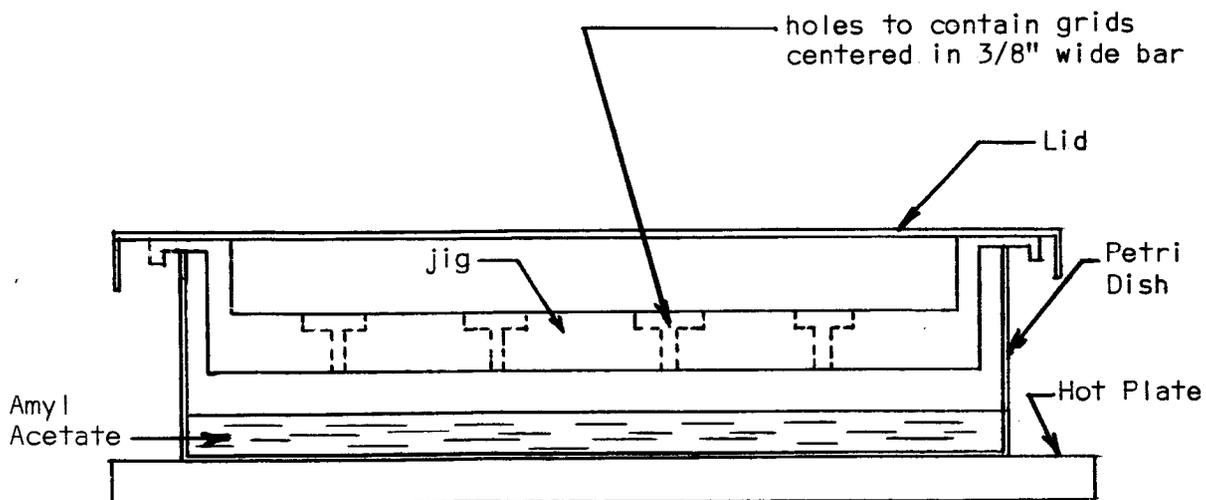
Figure 29
Washing Apparatus

The difficulty encountered with this method is that the Scotch Tape will not dissolve away from the grid readily and hence one is left with collodion and tape on the grid which becomes "trash" or "dirt" when examined in the electron microscope. This can be overcome by cutting a very small hole in the tape (smaller than the size of the grid) and placing this small hole over the center of the grid when applying the tape.

Some difficulty is also encountered in stripping the collodion off the silicon surface. This may be overcome by breathing heavily on the collodion surface until a slight moisture condensate forms. Then apply the tape and proceed with the stripping process.

Vacuum Evaporation of Carbon

The apparatus used for the vacuum evaporation of carbon is shown in Figure 30 in simplified form.
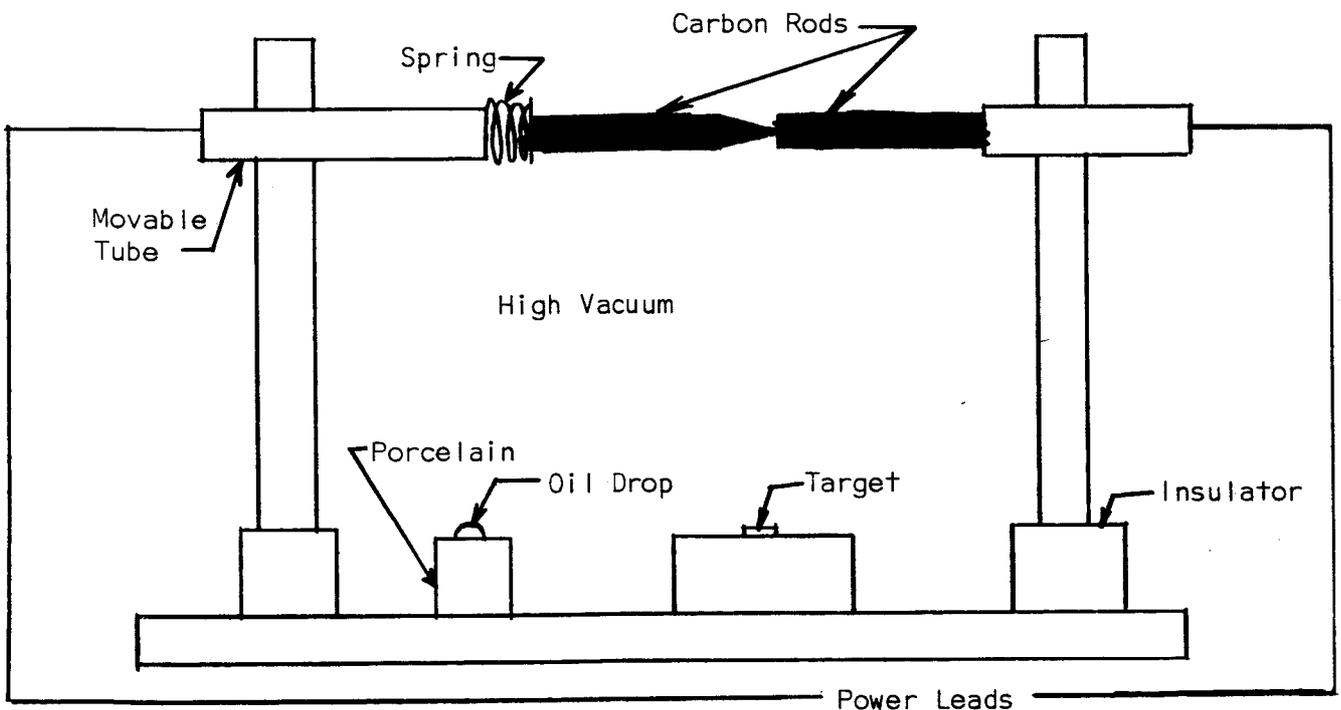
Figure 30
Carbon Evaporation Unit

-60-

The unit used is the JEE-4B Vacuum Evaporator manufactured by Japan Electron Optics Laboratories Co., Ltd. The apparatus has the following features:

1. As the bell jar is furnished with two independent electrodes, one with a pair of filament holders and the other with a pair of filament holders and of carbon holders, two different kinds of metals can be evaporated successively, or carbon evaporation and metal evaporation can be performed at the same time or successively, by proper use of these holders.

2. The highly efficient oil diffusion pump and the rotary pump are used for keeping a vacuum less than 10^{-5} mm Hg. Furthermore, pre-evacuation can be performed through the by-pass valve so that vacuum will be restored to the degree above immediately after exchange of a specimen.

The procedure is as follows: Two hard carbon rods are mounted in insulated holders. The blunt one is fixed and the pointed one is movable. A spring maintains a light pressure at the points. The target is placed about 10 cm from the source. A thickness indicator, consisting of a piece of white porcelain with a drop of vacuum oil on it is placed beside the target. The apparatus is covered with a bell jar and evacuated to between 10^{-4} to 10^{-5} torr. The carbon is now evaporated. The best thickness is believed to be obtained on this apparatus by passing 50 amps for a time of thirty seconds. The thickness is judged by the brown coloration on the indicator. This is visible on the area of the porcelain not covered with oil. When the brown color is just detectable compared to the white of the oil-covered area, the thickness of the film on the target is about 50 Å. Other thicknesses will be experimented with to try to obtain the optimum. This would be the

thinnest carbon film which could be obtained and which would still hang

together. Naturally the thicker the film, the poorer the resolution.

Shadow Casting

Shadow casting is a technique which consists of depositing by vacuum

evaporation a layer of electron-dense material onto the specimen at an angle.

(Figure 31)
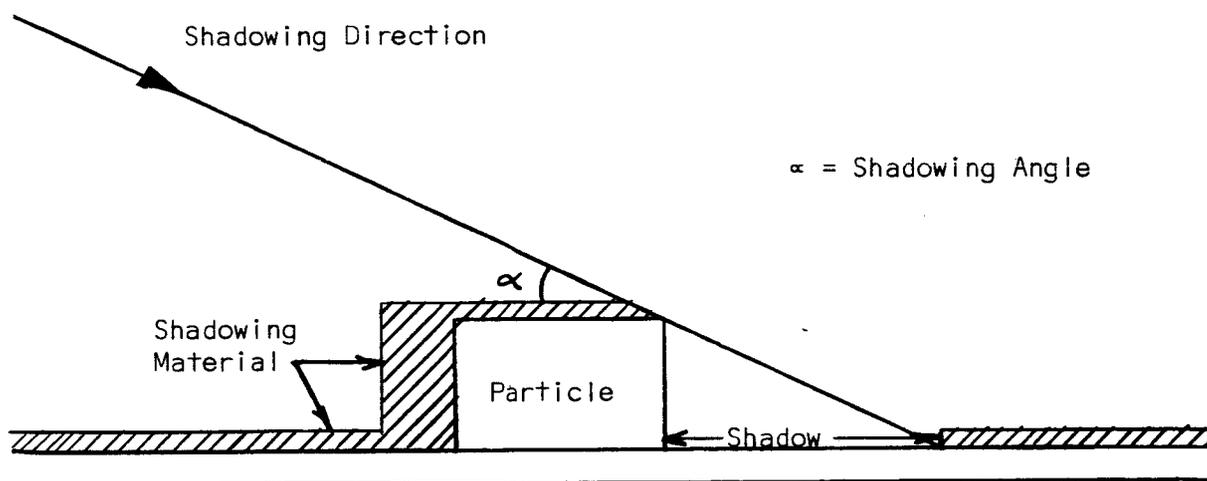
Figure 31
Shadow Casting

The areas shielded from the impinging beam of atoms by surface

irregularities are not coated. These areas are more electron-transparent than

the coated areas and resemble shadows in appearance. When examined in the

electron microscope, they will appear lighter than the surrounding areas.

When a micrograph is taken of such a specimen the images of the shadows are

reversed and appear dark, thus giving the impression of a surface illuminated

obliquely by white light. A print is then made which reverses this and gives the same picture observed in the microscope. The main purpose here is to provide added contrast to the final image produced by the electron microscope. Also by knowing the angle of deposition, it is possible to determine the height or size of surface projections or to determine their shape by the length of the shadows.

Up to this stage in the project platinum has been the shadowing material. This is accomplished very easily in the JEE system described previously. Shadowing has been done by evaporating a short piece (about 1 inch) of 8 mil platinum wire wrapped around a tungsten filament by heating to 36 amps for 30 seconds. This method works fine now, but later when very high magnification is required it is believed that the platinum will show a granular structure. This will be overcome by using platinum/carbon shadowing. This method should be capable of very high resolution and cause only very fine background structure. The platinum and carbon are evaporated simultaneously to form a deposit which has a high electron scattering power, but does not form discrete crystallites associated with evaporated films of heavy metals. The method depends on the use of rod type electrodes consisting of a mixture of platinum and carbon. However, it is believed that equally good results can be obtained by using carbon rods in a set-up like Figure 30 and wrapping platinum wire on one of the electrodes. The angle of incidence should be very small, about five degrees. This method will be put to use when a high degree of magnification is desired.

V.   Fundamentals of Photo Resist Materials

   A.   Introduction

      The silicon-silicon oxide interface properties in production devices
are intimately related to photo resist portions of the manufacturing processes.
Application of the fundamental information sought in this program will require
understanding the influence of the photo resist processing. This section
summarizes the results of an initial literature study of the chemistry and
technology of photo resist materials.

   B.   General Information

      Two basic types of photo resist, a positive and a negative type,
exist. The positive type produces a positive image of the original drawing
upon development, where the negative type produces a negative image of the
original drawing. Therefore, if a film coated substrate is to have its
remaining film (after etching) identical to the inked lines of the drawing
and if the foil is coated with a negative resist, then a negative of the
inked drawing must be used to expose the photosensitive resist.

      The most popular photosensitive resists in the electronics field
are currently those products by the Eastman Kodak Co. (KMER, KTFR, KPR).
Other resists (except AZ-1350, S-C grade from the Shipley Co.) are more
commonly used or proposed to be used in various lithographic processes.
Originally Kodak's photo resists were meant to revolutionize the printing
industry; however, the electronics industry adopted the products. Now the
three Kodak photo resist products, KPR, KMER, and KTFR (negative types), are
the leading resists, respectively, in the copper foil coating applications,
in the metal etch applications and the silicon shaping applications.

The positive photo resist available from the Shipley Co. may be satisfactory for metal etch operations (in particular semiconductor application) if it is desirable to eliminate the additional step of producing a negative of the original drawing. It would seem that further comments can be made only for specific cases since major semiconductor firms have chosen to remain with the negative photo resist processes. A major factor is the costly prospect of art work change-over.

The remaining photosensitive resist applications that appear in the literature seem to apply more to the printing trade. The basic spread of chemistry for these various photosensitive resists seems to be as follows: (1) the majority of these resists use some combination of polyvinyl alcohol (PVA), (2) Diazo Azide, Polyvinyl Cinnamate compounds, and phthalates of Hydroxy-containing polymers as the remaining basic building blocks.

Woodward, Chambers, and Cohen provide quite a useful insight((in their article, "Image-Forming Systems Based on Photopolymerization) into the chemistry and photographic characteristics of the photopolymerization. Some of the main points are as follows:

(1) Photopolymerization (first reference to it in 1945 by Gates) is outstanding as a result of its potential amplification, short access time, short chemical processing, stability, and versatility aspects. The spontaneous amplification of this widely studied system of photochemical image formation results in a high chemical quantum yield through a chain reaction in which a monomer, M, is converted to a polymer, $(M)_n$ in the following reaction:

$$nM \xrightarrow{\ h\nu\ } (M)_n$$
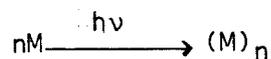
where n, the kinetic chain length, roughly approximates the quantum yield.

(2) The speed of a photographic system is determined by its overall utilization of information bearing incident light to record and detect this recorded information. Very high speed systems might result if the quantum yields are on the order of 10^6 and 10^9 (i.e. a polymerization yield of 10^6 monomers per photon absorbed). As of 1963 the best that had been obtained was about 10^3. However, chain lengths up to 10^8 are obtainable in addition polymerization. Addition polymerization does require special monomers, elimination of induction periods and rigorous control of inhibitors.

(3) Quite a bit of information is still lacking; such as the complete chemistry of photopolymerization (a) for excited states; (b) for mechanisms for energy transfer and radical formation, and (c) for the relationship of polymerization reactions to physical property changes.

(4) The primary chemical step is photoinitiation which occurs when an initiator component absorbs radiation at some wavelength between 2000 and 7000 $\overset{o}{A}$ to form an excited species capable of generating a polymerization-initiating free radical. This excited species (the same molecular structure, but now more energetic) as compared to the unexcited species is potentially capable of many reactions. The photon's energy causes a rearrangement of the electrons involved in the formation of chemical bonds and results in many paths by which the energy of such excited molecular states may be dissipated or utilized.

(5) The polymerization takes place when molecules at an excited state produce polymerization initiating radicals.

(6) An antihalation coating can decrease undesirable photopolymerization
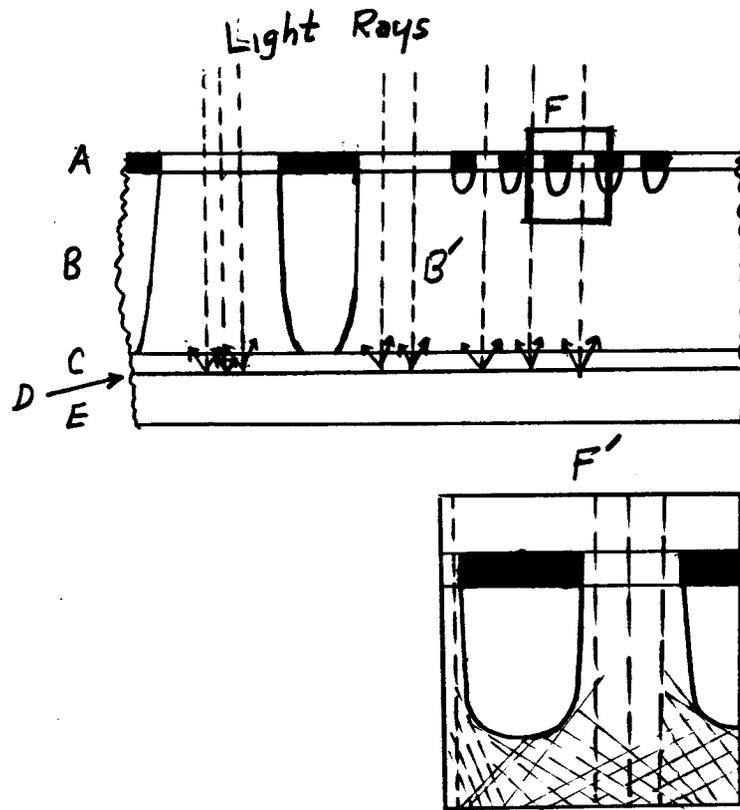
Figure 32
Photopolymer Cross Section During Exposure

(A) Film negative
(B) Photopolymer layer, (B') Exposed (insoluble) polymer layer
(C) Non-sensitive bonding layer
(D) Anti-halation coating
(E) Steel Support (substrate)
(F & F') Section and cross section (underexposed)

since reflections otherwise blur the film negative image impressed upon the

light-sensitive polymer. (See Fig. 32)

It is now possible to appreciate the general aspects of the presently

existing photo resist materials.

C. KMER and KTFR

1. General Chemical Structure

These trademarked products of Eastman Kodak Company are more

completely titled Kodak Metal Etch Resist and Kodak Thin Film Resist.

Eastman Kodak Co. has not supplied any chemistry particulars other than

application information, some of the latter dated as late as 1964, and as a

result a considerable amount of literature search has been necessary in order

to establish a reasonable basis for chemical understanding of KMER and KTFR.

The details are now presented.

KTFR is a refinement of KMER. KMER has previously been "cleaned

up" at least by a centrifuge process for high resolution applications. KMER

may be thought to be very close to 3- and 4- (α-cyanocinnamido) phthalates of

hydroxyl-containing polymers. The following information came from personal

communications, the Patent Gazette, and Chemical Abstracts.

The sections B and C, Fig. 33a and the sections B and C, Fig.

33b, can be identical. However, section A, Fig. 33, is polyvinyl cellulose.

It is necessary to consider further the patent 2,861,057 information from

the Gazette, the Chemical Abstracts, and personal communications. Since

the patent information and other sources hint that section A is polyvinyl

alcohol, KMER and KTFR may be supposed to have PVA as section A of the

chemical structure (See Fig. 33). Since the patent 2,861,057 (filed

December 17, 1956 and granted November 18, 1958) is the latest of the series
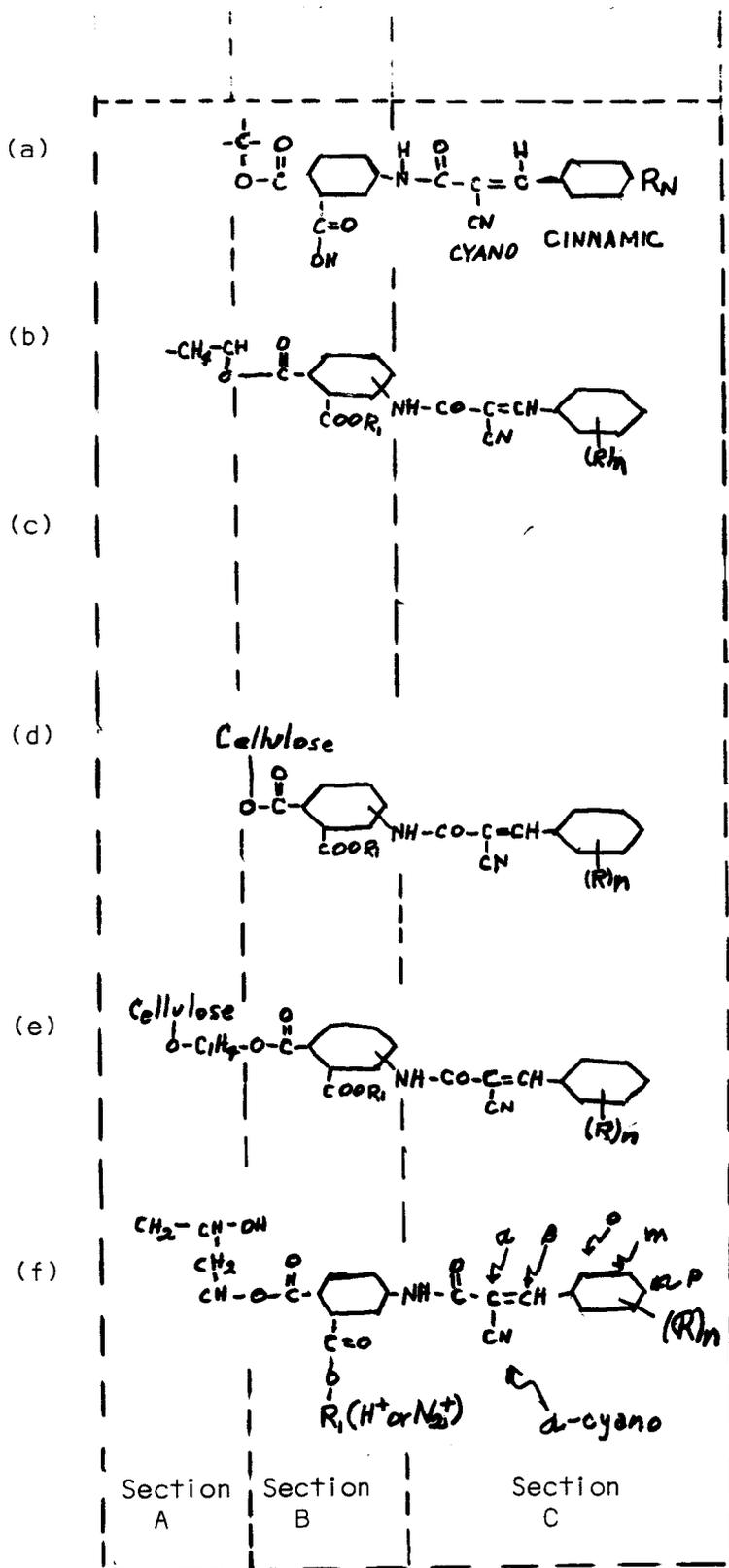
Figure 33
Photosensitive Resist Chemical Chains

(a) Partial KMER chain
(b-e) Chains in Merrill Patent
(f) Complete general KMER, KTFR chain

of light sensitive polymer patents:

2,835,656 filed November 25, 1953

2,848,328 and 2,852,379 filed May 4, 1955

2,861,058 filed July 29, 1955

2,865,750 filed March 18, 1955

(issued before the KMER trademark 752,504 and granted November, 1958, (trade-
mark use date January 4, 1960, and filing date September 20, 1962), and it
describes light sensitive polymers of 6,000 times the sensitivity of poly
(vinyl cinnamate), this latter mentioned in patent application 2,865,750;
then there exists a reasonable basis for belief that KMER and KTFR have the
basic chain of Fig. 33 (originally described in patent 2,861,057).

The KMER, KTFR chemistry can be a variation of the basic patent
since the take-off from the benzene rings are in a flexible configuration.
This general configuration allows possible later refinements for more desirable
characteristics.

2. Specific Chemical Structure

The general patent (14) comments about the structural chains are
as follows:

"3- and 4- (α-cyanocinnamido) Phthalates of Hydroxyl-containing
polymers (can be) I. A resinous polymer selected from the group consisting
of (1) a vinyl polymer consisting of at least 30% by weight of the recurring
general structural unit: (Fig. 33) wherein n represents an integer of from
1 to 2 and R represents a member selected from the group consisting of a
hydrogen atom, a chlorine atom, a bromine atom, an alkyl group of 1 to 4
carbon atoms, an alkoxy group of 1 to 4 carbon atoms, an acetamido group, a

-COOR$_1$ group, an -SO$_3$R$_1$ group and an (Fig. 33) group and wherein in each

instance R$_1$ represents a member selected from the group consisting of a hydrogen

atom and an alkali metal atom and R$_2$ represents an alkyl group of 1 to 4 carbon

atoms, the remainder of the polymer molecule to make a total of 100% being

composed of residual recurring structural units selected from the group con-

sisting of a vinyl alcohol unit, a vinyl ester of a saturated monobasic fatty

acid of 2 to 4 carbon atoms unit, and vinyl alcohol and said vinyl ester units

in linear combination, (2) a cellulose ester consisting of at least 30% by

weight of the recurring general structural unit: (Fig. 33) wherein $\underline{n}$, R and

R$_1$ are as above defined, the remainder of the cellulose ester molecule to

make a total of 100% being cellulose acetate units, and (3) a cellulose ether

consisting of at least 30% by weight of the recurring general structural unit:

(Fig. 33) wherein $\underline{n}$, R and R$_1$ are as above defined, the remainder of the

cellulose ether molecule to make a total of 100% being hydroxylethylcellulose

units."

The phthalate group (Fig. 33, section B) and α-cyanocinnamide

group (Fig. 33, section C) may be attached either to Polyvinyl Cellulose or

Polyvinyl Alcohol. The Chemical Abstractor for this patent outlines the

procedure for the polyvinyl alcohol combination.

3. Properties

KMER and KTFR are essentially the same type of honey-colored,

light sensitive resist. Both resists are low molecular weight compounds

that use the same chemical processing techniques. KMER differs by the fact

that it has an observable graininess in its KMER bottle (This graininess has

caused its users to refer to it as "applesauce". The graininess supposedly

stems from a particular statistical frequency distribution of polymer length). The ash content of KTFR is kept under .0003% so that very high resolution is possible. KMER is recommended for thick coatings of resist since the exposure time for KTFR may be excessive (for a coating thickness of 0.0003 inch or greater). KMER single-coat thickness may range to 0.001 inch.

KMER was basically designed for aluminum, tool steel, stainless steel, titanium, and other structural metals; however, semiconductor use has increased its use to include germanium, molybdenum, tantalum, silicon, nickel, and (with additives) glass, and silicate surfaces. KMER can also be used for gold, magnesium, copper, nichrome, zinc, silver and plastics not attacked by aromatic hydrocarbons. KPR is preferred for copper.

KMER and KTFR will resist acids such as HNO_3, H_2SO_4, H_3PO_4, HF, some alkaline solutions such as NaOH, and water as a solvent. Hot chromate acid $+H_2SO_4$ will remove the resists but other resist-strippers may be preferred or required such as Litho Aluminum Products Company's Resist-Strip J-100 or boiling C_2HCL_3. Chromate acid may adversely coat glass surfaces.

KTFR may adhere also to the same materials as KMER but the resolution requirement is the governing factor in the choice between KMER and KTFR resists. Heating of the resist should be limited to a temperature of 100°C. Adhesion will rise when heated until there is a color change from honey to milky-white. Past this point adhesion will drop to 10%. Excessive heating can cause a developed image to flow.

KMER, KTFR photo sensitivity extends into the visible light region so that an incandescent light source, even through certain glass,

will cause photopolymerization to take place.

Irradiation produces cross-linking so that the image remains upon development.

Note that for R_1 (Fig. 33) being a N_a salt then the KMER, KTFR compound is basic and tends to be more water soluble. If R_1 is a free acid (H+) then the KMER, KTFR compound tends to be more soluble in organic solvent.

4. State-of-the-Art Techniques

Both resists must be applied to clean surfaces if undercutting due to poor adhesion is to be avoided. Sometimes if adhesion difficulty still prevails then either bake resist longer (at 100°C) after development stage or (1) use Kodak's additive D (for glass and ceramic), (2) use a fluorocarbon non-ionic surface wetting agent (Minnesota Mining and Manufacturing Company's L1060) with the resist in silicon or silicon-oxide applications.

KTFR has a much higher resolution than KMER (KMER tends to fuss), the good resolution of KTFR permitting circuit elements of 1/2 micron separation. However, a limit of an element of 1 micron in width using KTFR seems to be the present case for one large semiconductor manufacturer. This limit of 1 micron seems to be a result of interference, bars and rings, that begin to appear; possibly as a result of the physical optics associated with the small apertures of the mask. Image reduction (via a lens system) during photo resist exposure is to be avoided where good overall replication is desired. Substrate indexing using a steromicroscope (of at least 40X magnification) and a precise X-Y maneuverable chuck can give good replication as compared to the use of a fly's-eye lens system or a series of grid lines.

Humble Oil Company's Varsol works as a satisfactory substitute for Stoddard solvent developer . Use of alcohol instead of xylene prevents

-73-

accidental resist swelling. Resist coatings are best when a spin operation
is employed to smooth the coating.

Addition of Stannous salts to photo polymerizable compositions
decreases undercutting, and increases adhesion and image quality.

For good microcircuit replication every step must be completed
under identical conditions. Masks may need to be from a drawing up to
500 times larger. Also, masks may need to be etched glass in order to
maintain high dimensionable stability. Mask image must be adjacent to the
substrate resist film and must be aligned and exposed by light rays
having the same angle of incidence on the substrate plane (90°). Higher
magnification with good definition can be obtained. A simple mask can also
be made to produce several images.

The stripping of polymerized films (recommended by Keonjian)
is by boiling in C_2HCl_3 (trichloroethylene) then by "scrubbing" in acetone
or heating in mineral acids such as HNO_3 or H_2SO_4. Litho Products suggests
their resist strip J-100.

D. Conclusion

The opportunities for extraneous materials to be included in a
thin layer of oxide are numerous. Detailed analysis of surface chemical
composition may be required to determine the influence of these materials
on the properties of the Si/SiO_2 interface.

VI. Analytical Equipment

A. Electron Mirror Microscope of Litton Industries

A visit to the Litton facility in Minneapolis revealed that the readily obtained maximum direct magnification with existing instruments is 3700X. For 0.37 mm as the minimum satisfactory spacing on the recording film, the minimum specimen resolution is 10^{-7} m or 1000 Angstroms. Conversation with men working on the machine indicated that one to three years will be required for them to have studied the machine sufficiently thoroughly to have a definite indication of their capability on a project similar to the Si/SiO_2 interface study.

A few specimens should be submitted to them each year to determine if useful information can be obtained by the electron mirror approach.

B. Fluorescence Analysis

Pursuit of analysis techniques for highly purified water may have led to an analysis technique with broad applications. The initial consideration was for a sensitive, convenient, and inexpensive indication of impurities in deionized water. The "ideal" approach being a device from which one can extract an electrical signal indicative of the impurity content. Such an electrical approach contrasts readily with the common techniques, usually requiring wet chemical analysis.

The electrical conductivity measurement on water gives the ionic conduction quite readily. Suspended inorganic solid materials and both dissolved and suspended organic materials do not contribute to ionic conduction. Other analytic techniques used include:

for Suspended Solids - residual mass after evaporation

                            - flow stoppage in a fine filter

for Organic Content - concentration, oxidation, and titration

                            - bacteria count

None of these are conveniently performed in anything less than a well equipped analytical laboratory. An electrical analytical technique offers much convenience.

Fluorescence in a material depends on the existence of certain relative energy levels for electrons around the atoms and appropriate electronic transition properties. Operationally, fluorescence is the excitation of material atoms at one wavelength of light with re-emission of radiation at another wavelength, usually a longer wavelength. Most organic materials fluoresce to some degree and a small fraction of inorganic compounds fluoresce. The best known examples of the latter are the natural minerals which fluoresce.

Research scientists in the life sciences have come to use the unique and powerful analytic capabilities of fluorescence phenomena. An extremely large number of organic molecules have unique fluorescence spectra just as some have unique infrared or ultraviolet absorbtion spectra. Because the kind of fluorescence spectrum of a material depends on the wavelength of the excitation radiation, fluorescence analysis has another dimension over the ordinary absorbtion spectrum techniques. Fluorescence can be an exceptionally powerful analytic phenomenon in many cases. For those materials which do not fluoresce, it obviously has no analytical value.

Deionized water systems can be installed and filtered to have

extremely low inorganic impurity content. The plumbing is organic, the

deionizing resin is organic, and the most difficult of materials to remove

from the raw water are the dissolved organics. Fractions of all these

organics can be in the deionized water of a well-managed purification system.

The concentrations are sufficiently low and the common analytical techniques

so cumbersome that little is usually done to monitor this source of ex-

traneous material in semiconductor device production.

A selected list of references has been examined to estimate how much

information exists about the probable success of using fluorescence to monitor

deionized water purity in conjunction with the usual ionic conductivity

measurement:

Sidney Udenfriend, Fluorescence Assay in Biology and Medicine,
Academic Press, 1962.

Gerald Oster and A. W. Pollister, eds., Physical Techniques in
Biological Research, vol. III, Academic Press, 1956.

P. Pringsheim, Fluorescence and Phosphorescence, Interscience, 1949

C. A. Parker, "Raman Spectra in Spectrofluorometry," The Analyst 84,
446 (1959).

Relatively few compounds have been thoroughly indexed for fluores-

cence analysis. Present research workers are contributing to a growing

body of data.

A research investigation must be performed to isolate the primary

organic constituents and the wavelength bands best for excitation and

observation of the dominant impurities. Then a relatively simple filtered

source exciter and filtered beam detector could give a quite meaningful

relative indication of the quantity of organic material in the water and

whether the level is constant with time. Water has fluorescent bands of its own which prevent operation at those wavelengths, but this property offers an easy means of calibration for light source, optics, and electronics of the measurement system. A combination instrument for conductivity and fluorescence analysis can be compact and simple to use. The cost should be moderate. Such monitoring instruments can be put on each production line for indicating the quality of water used and the results of washing operations at critical steps in device manufacture. This appears to be a useful way of improving quality control on high reliability devices.

Instruments on the market can be readily adapted to such application. Manufacturers include

American Instrument Company
8030 Georgia Avenue
Silver Spring, Maryland

G. K. Turner Associates
Palo Alto, California

Farrand Optical Company
Bronx Boulevard and East 28th Street
New York 70, New York.

To obtain the information around which meaningful specifications for water could be written, a nine to twelve month program of water evaluation combined with device evaluation should be executed. A double monochromator instrument (with recorder) for precise analysis costs about $7,000. An instrument using interference filters as the monochromators can be purchased for less than $2,000. Use of these instruments in conjunction with other device research should produce very useful quality control specifications.

APPENDIX

Table 1

100 cps	Volts	Capacitance	Conductance
	0.10	116.10	0.0154
	0.30	93.18	0.0069
	0.50	79.48	0.0055
	1.00	61.37	0.0035
	3.00	40.43	0.0012
	5.00	29.30	0.0011
	10.0	22.20	0.0007
	30.0		
	50.0	unable to get indication	

Table 2

1000 cps	Volts	Capacitance	Conductance
	0.10	131.46	0.0960
	0.30	87.26	0.0366
	0.50	75.20	0.0267
	1.00	59.05	0.0156
	3.00	37.30	0.0057
	5.00	29.81	0.0037
	10.0	21.91	0.0027
	30.0	13.40	0.0022
	50.0	10.20	0.0019

Table 3

10,000 cps	Volts	Capacitance	Conductance
	0.20	88.38	0.0110
	0.30	81.30	0.0100
	0.50	70.02	0.0087
	1.00	56.21	0.0073
	3.00	36.30	0.0063
	30.0	11.14	0.005
	50.0	10.10	0.005
	100.0	10.09	0.005

BIBLIOGRAPHY

1. B. E. Deal, A. S. Grove, E. H. Snow, C. T. Sah,
    "Recent Advances in the Understanding of the Metal-Oxide-Silicon
    System,"
        Presented at the AIME Conference on Electronic Materials, Boston,
        September 1, 1964.

2. J. E. Thomas, Jr. and D. R. Young,
    "Space-Charge Model for Surface Potential Shifts in Silicon Passivated
    with Thin Insulating Layers,"
        IBM Journal of Research and Development, Vol. 8, No. 4, pp. 368-375,
        September, 1964.

3. H. H. Skilling,
    Electrical Engineering Circuits, New York, John Wiley & Sons, pp. 18-20,
    1959.

4. L. P. Huselman,
    Circuits, Matrices, and Linear Vector Spaces, New York, McGraw-Hill
    Book Co., Inc., pp. 3-5, 112-113, 1963.

5. D. N. Chorofas,
    Statistical Processes and Reliability Engineering, New York, D. Van
    NostrandCo., Inc., pp. 11-14, 1960.

6. "Operating Instructions Type 1615A Capacitance Bridge,"
        General Radio Company, West Concord, Massachusetts, October, 1963.

7. Personal Communication,
        Stan Gessel, Product Specialist, Electro-scientific Industries to
        Dr. H. Lyndon Taylor.

8. "Instruction Manual Electro-scientific Industries Model 277 Capacitance
    Bridge,"
        Electro-scientific Industries, Portland, Oregon, April, 1963.

9. P. J. Holmes,
    The Electrochemistry of Semiconductors, New York, Academic Press,
    1962.

10. Lee Barnes,
        Private communication.

11. Karl H. Kretzer,
    "Positive Working Photoresist Layer,"
        Chemical Abstracts, Vol. 60, No. 2, p. 1265, January, 1964.

12. Andre K. Schnerin and H. D. Evans,
         "Photographic Polymeric Resist Images,"
            Chemical Abstracts, Vol. 60, No. 2, p. 1266g, January, 1964.

13. P. W. Woodward, V. C. Chambers, A. B. Cohen,
         "Image-Forming Systems Based on Photopolymerization,"
            Photo. Science Engineering, Vol. 7, No. 6, pp. 360-368, 1963.

14. Stewart H. Merrill and Donald A. Smith,
         "Light-Sensitive 3- and 4- (α-Cyanocinnamoylamino) Phthalates of
          Hydroxy-Containing Polymers,"
            Chemical Abstracts, Vol. 53, p. 4989c, March, 1959.

15. W. E. Rowe,
         "Photographic Fabrication of Semiconductor Devices,"
            Chemical Abstracts, Vol. 58, p. 12069a, June, 1963.

16. Cornelius C. Unruh and D. A. Smith,
         "Light-Sensitive Polymers for Photography,"
            Chemical Abstracts, Vol. 53, 1959.

17. Cornelius C. Unruh, G. W. Leubner, A. C. Smith, Jr.,
         "Light-Sensitive Polymer for Printing Plates,"
            Chemical Abstracts, Vol. 53, p. 4991e, March, 1959.

18. E. Keonjian (editor),
         "Microelectronics, Theory Design, Fabrication,"
            McGraw-Hill, New York, New York, pp. 184, 177-178, 290-296, 1963.

19. Eastman Kodak Co., Rochester, New York,
            Industrial Data Handbook, p. 7, 1962, 1964.

VII. General Bibliography Section

This bibliography was assembled from the NASA Scientific and
Technical Aerospace Reports (STAR) Abstract Journal. This section is
an addition to those in the previous report.

Bibliography

on the

Silicon Interface

prepared as a portion of the

Physical Science of Reliability Program

at the

Electronic Materials Research Laboratory

Department of Electrical Engineering

The University of Texas

under the sponsorship of the

Applied Physics Branch

Astrionics Laboratory

George C. Marshall Space Flight Center

National Aeronautics and Space Administration

Huntsville, Alabama

THE NASA SCIENTIFIC AND TECHNICAL AEROSPACE REPORTS

(NASA STAR)

Each of the entries listed is preceded by the NASA accession number

(e.g. N63-10000) followed by a category number (e.g. 10-07) for locating the

abstract in the STAR publication. The first two digits of the category num-

ber indentify the issue number and the last two digits identify the category

as listed in the Table of Contents of NASA STAR. The accession number is

followed by the originating organization's report number and a Defense

Documentation Center number, where available.

N63-10183-01-15, AMRL-TDR-62-88,
   M. J. Allen,
      "Calibration of the Infrared Optometer. Technical Documentary Report
      (May 1, 1961 - March 13, 1962),"
         August, 1962, Contract AF33(616)-6146

N63-10282-01-18, DMIC-MEMO-160,
   C. H. Lund, H. J. Wagner,
      "Identification of Microconstituents in Superalloys,"
         November 15, 1962, Contract AF33(616)-7747

N63-10367-01-25, AROD-2838-1,
   A. M. Goodman, W. W. Mehl,
      "Research on Metallic Contacts to Semiconductors. Final Report for
      the Period June 23, 1960 to June 22, 1962,"
         July 26, 1962, Contract GA-034-ORD-3282RD

N63-10410-01-09, NBS-TN-201,
   R. N. Jones,
      "A Technique for Extrapolating the 1 KC Values of Secondary
      Capacitance Standards to Higher Frequencies,"
         November, 1963

N63-10498-01-23,
   A. M. Russel,
      "Tables of Non-Relativistic Electron Trajectories for Field Emission
      Cathodes,"
         October, 1962, Contract Nonr-1842(02)

N63-10507-01-25, AFCRL-62-772,
   M. M. Atalla, R. W. Soshea, R. C. Lucas, C. H. Fox, V. M. Dowles,
     "Investigation of Hot Electrons Emitter. Science Report No. 1,
     June 1 - August 31, 1962,"
       1962, Contract AF19(628)-1637

N63-10562-01-15, AFCRL-62-1070,
   E. N. Lassettre, F. M. Glaser, V. D. Meyer, A. Skerbele,
     "Recent Advances in the Use of the Electron Spectrometer,"
       September, 1962, Contract AF19(604)-4541

N63-10674-02-15, AEC-TR-5080,
   Heinz Ewald and Heimich Hintenberger,
     "Methods and Uses of Mass Spectroscopy,"
       July, 1962

N63-10759-02-25, AFCRL-62-585,
   M. K. Wilson,
     "Spectroscopic Investigations of Solid State Surfaces Containing
     Absorbed Molecules. Final Report,"
       May, 1962, Contract AF19(604)-4063

N63-10876-02-16, ARL/MET-15,
   T. Mills,
     "A Vacuum Microbalance for High Temperature Oxidation Studies.
     Metallurgy Note 15,"
       April, 1962

N63-11173-03-23, AFCRL-62-904,
   O. Heil and S. Vogel,
     "Surface Explosions on Solids by High-Density Electron Bombardment,"
       October, 1962, Contract AF19(628)-1606

N63-11239-03-01, WACC-TK-53-373, Supplement 9,
   D. J. Tate,
     "A Review of the Air Force Materials Research and Development
     Program. Final Report, July 1, 1961 - June 30, 1962,"
       November, 1962

N63-11691-04-15, BM-RI-6111,
   J. D. Brown, et. al.,
     "Design, Construction, and Evaluation of an Electron Probe X-Ray
     Spectrograph,"
       1962

N63-11803-04-15, AFCRL-62-933,
   T. O. Passell, J. B. Swediunst, et. al.,
     "Development of X-Ray Fluorescence Analysis Techniques for Small
     Samples: A Prototype Atmospheric Electron Probe - Final Report,"
       October 31, 1962, Contract AF19(604)-8827

N63-11843-04-07, JPRS-17176,
   L. A. Gribov,
      "Methods of Calculation in Molecular Spectroscopy,"
         January 17, 1963

N63-11952-05-09,
   D. R. Chambers,
      "Integration of Energy Storage and Discharge Mechanisms in Bulk
      Silicon and Germanium for Application in Neuristor Lines. Interim
      Report 6,"
         October, 1962, Contract Nonr-3112(00) and AF33(657)-7801

N63-12094-05-23, MRL-126,
   A. N. Goland,
      "The Role of Electron Microscopy in Observations of Radiation
      Damage,"
         November, 1962

N63-12184-05-23, DMIC-MEMO-161,
   W. R. Warke and A. R. Elsea,
      "Electron Microscopic Fractography,"
         December, 1962, Contract AF33(616)-7747

N63-12579-06-23,
   R. W. G. Wyckoff, F. D. Davidson,
      "Windowless Tubes for X-Ray Spectroscopy,"
         1962, NASA Grant NSG-120-61

N63-12643-06-25, AFCRL-62-949,
   H. E. Farnsworth, J. A. Dillon, Jr., et. al.,
      "Investigations of Surface Properties of Silicon and Other Semi-
      conductors. Final Report, October, 1959 - September 30, 1962,"
         November, 1962, Contract AF19(604)-5986

N63-12945-07-09,
   P. K. Weimer, H. Borkan, et. al.,
      "Evaporated Thin Film Devices. Scientific Report No. I, Period
      June I, 1962 to November 30, 1962,"
         November, 1962

N63-12988-07-23,
   F. D. Davidson, R. W. G. Wyckoff,
      "X-Ray Fluorescent Yields from Several Light Elements,"
         December, 1962, NASA Grant NSG-120-61

N63-13053-07-23, AROD-2588-3,
   M. P. Givens,
      "A Study of the Optical Properties of Solids in the Extreme Vacuum
      Ultraviolet and/or the Soft X-Ray Regions. Final Report, June I,
      1960 - October 31, 1962,"
         January 8, 1963, Grant DA-ORD-17

N63-13191-07-01,
   George C. White, Jr., et. al.,
      "Basic Research in Physical Sciences.   Second Quarter Progress Report
      for PY 63,"
         December, 1962

N63-13213-07-01,
   C. D. Thibault, ed.,
      "Materials Research Abstracts, A Review of the Air Force Materials
      Research and Development,"
         1962

N63-13593-08-15,
   A. M. Russell,
      "Field Emission Spectrometer, Technical Report No. 5,"
         December, 1962, Contract Nonr-1842(02)

N63-13796-09-23, AEDC-TDR-63-49,
   R. L. Heimburg, et. al.,
      "Measurement of Pressure in an Ultra-High Vacuum,"
         March, 1963, Contract AF40(600)-909

N63-13599-08-23,
   "Third International Symposium on X-Ray Optics and X-Ray Microanalysis,
   Stanford University, August 22-24, 1962,"
      Grant NSG-296-62

N63-14255-10-15, BM-RI-6212,
   F. D. Stevenson, C. E. Wicks,
      "A Metal Diaphragm Apparatus for Measuring Vapor Pressure. Vapor
      Pressure of Arsenic (III) Oxide,"
         1963

N63-14276-10-15, NASA TND-1695,
   M. M. Sokoloski, F. E. Geiger,
      "Apparatus for the Measurement of Transport Properties of Polar
      Semiconductors,"
         1963

N63-14294-10-18, USBM-U-1001,
   A. H. Roberson, et. al.,
      "Quarterly Metallurgical Progress Report No. 17 for the Period of
      October 1 through December 31, 1962,"
         Contract AT(11-1)599

N63-14412-10-25, AEC-TR-4475,
   S. I. Pekar,
      "Research in Electron Theory of Crystals,"
         February, 1963

N63-14533-10-09, AFCRL-63-21,
   H. W. Cooper, et. al.,
      "Research and Development for Surface Protection for Silicon Devices,
      Scientific Report No. 3, June 15 - September 14, 1962,"
         October, 1962, Contract AF19(604)-8358

N63-15161-11-25,
   W. J. Fredericks, F. J. Keneshea, F. Craig,
      "A Bibliography of Group I-VII Elements and Their Compounds, Volume I
      Scientific Report No. 2,"
         1946-1961, Contract AF19(604)-7231

N63-15162-11-25,
   W. J. Fredericks, F. J. Keneshea, F. Craig,
      "A Bibliography of Group II-VI Elements and Their Compounds, Volume II
      Scientific Report No. 2,"
         1946-1961, Contract AF19(604)-7231

N63-15163-11-25,
   W. J. Fredericks, F. J. Keneshea, F. Craig,
      "A Bibliography of Group III-V Elements and Their Compounds, Volume III
      Scientific Report No. 2,"
         1946-1961, Contract AF19(604)-7231

N63-15164-11-25, AFCRL-62-917(IV),
   W. J. Fredericks, F. J. Keneshea, F. Craig,
      "A Bibliography of Group IV Elements and Their Compounds, Volume IV
      Scientific Report No. 2,"

N63-15802-13-25, NOLTR-62-125,
   D. F. Bleil, et. al.,
      "Solid State Research of the Applied Physics Department for the Year
      1961,"
         July 16, 1962

N63-15960-13-20, LMSC-6-90-63-23,
   H. P. Greinel,
      "Diffraction Pattern Analysis of a Rectangular Aperture in the
      Presence of Aberrations Part 2:   The Diffraction Pattern in the
      Presence of Single Third-Order Aberrations: I.   The Effect of
      Primary Astigmatism,"
         May, 1963

N63-16106-13-25, RADC-TDR-63-30,
   S. M. Skinner, J. W. Dzmianski,
      "Study of Failure Mechanisms. Final Report, July 1, 1961 to
      September 30, 1962,"
         December, 1962, Contract AF30(602)2558

N63-16144-13-07, UCRL-7238,
   J. E. Senkin and M. I. Milliken,
      "Absorption Spectra of Various Metallic Halides and Oxides,
       Elemental Carbon and the Inert Gases: A Bibliography,"
          February, 1963, Contract W-7405-eng-48

N63-16978-14-23, BM-IC-8166,
   Howard M. Stainer,
      "X-Ray Mass Absorption Coefficients, A Literature Survey,"
          1963

N63-17083-15-25, AFCRL-62-949, Supplement,
   J. A. Dillon, Jr. and R. M. Oman,
      "Investigations of Surface Properties of Silicon and Other Semi-
       conductors. Final Report, 30 September, 1962 - 31 January, 1963,"
          February, 1963, Contract AFI9(604)-5986

N63-17351-15-09, ONR-14,
   "Proceedings of Second Conference on the Navy Microelectronics Program,
    Washington D.C., September 24 - 26, 1962,"
       1963

N63-17388-15-25, AFCRL-63-113,
   "Investigations of Hot Electron Emitter - Scientific Report No. 3,
    December 1, 1962 - February 28, 1963,"
       Contract AFI9(628)-1637

N63-17608-16-25, AFCRL-63-65,
   F. Euler and G. H. Schwuttke,
      "Dislocation Studies in Diamond By X-Ray Diffraction Microscopy,"
          March, 1963

N63-17902-16-15, AID-T-63-86,
   A. I. Akishin, V. S. Zozulin,
      "Film Thickness Control by Means of a Crystal Resonator,"
          1963

N63-18400-17-25, NASA CR-50456,
   F. R. Brotzen,
      "Physics of Solid Materials. Semiannual Status Report, November 1,
       1962 - Arpil 30, 1963,"
          NASA Grant NSG-6-59

N63-18640-17-09, RADC-TDR-63-152,
   K. Greenough, F. Reed, and N. Johnson,
      "Study of Failure Mechanisms at Surfaces and Interfaces,"
          March, 1963, Contract AF30(602)-2593

N63-18853-18-25, ORNL-3364,
   "Solid State Division Annual Progress Report for Period Ending August
   31, 1962,"
      November 15, 1962, Contract W-7406-eng-26

N63-19432-19-09,
   C. E. Horton, J. W. Hall, II,
      "Research, Development, and Fabrication of Tunnel Emission Cathodes.
      Second Quarterly Interim Technical Report, October - December, 1962,"
         1962, Contract DA-49-186-OKD-105

N63-19713-19-18,
   K. Lucke,
      "Recrystallization of Single Crystals. Third Quarterly Technical
      Status Report, December 1, 1962 - Febraury 28, 1963,"
         Contract DA-91-591-EUC-2438

N63-19717-19-18,
   P. P. Dennis and J. S. Brammar,
      "The Preparation of Thin Metal Foils by Microtomy: An Assessment of
      the Technique and its Application to Metallurgical Investigation
      with the Electron Microscope. Final Technical Report, December 31,
      1961 - March 30, 1962,"
         April 22, 1963, Contract DA-91-591-EUC-1695

N63-19805-19-25, AROD-1176-20,
   G. A. Jeffrey,
      "Research and Development of Electron Density Distribution in Semi-
      conductors. Final Technical Report, January 1, 1961 - December 31,
      1962,"
         Grant DA-ORD-31-121-61-G63

N63-20122-20-09, AERE-M-903,
   A. R. Owens,
      "The Behavior of Semiconductor Diodes in Pulse Applications,"
         January, 1962

N63-20-145-20-15, AROD-3975-1,
   Grahm Gurr,
      "A Normal Beam Automatic X-Ray Diffractometer,"
         June 20, 1963, Contract DA-ARO(D)-31-124-G412

N63-20230-20-25, ORNL-3480,
   "Solid State Division Annual Progress Report for the Period Ending
   May 31, 1963,"
      August 23, 1963, Contract W-7405-eng-26

N63-20267-20-18, DMIC-MEMO-161,
   W. R. Warke, A. R. Elsea,
      "Electron Microscopic Fractography,"
         December 21, 1962, Contract AF33(616)-7747

N63-20283-20-25, DS-117,
   M. Neuberger,
      "Silicon: Absorption Data Sheets,"
         December, 1962, Contract AF33(616)-8438

N63-20287-20-25, DS-120,
   M. Neuberger,
      "Silicon: Mean Free Path Data Sheets,"
         January, 1963, Contract AF33(616)-8438

N63-20289-20-25, DS-126,
   M. Neuberger,
      "Silicon: Electrical Conductivity Data Sheets,"
         June, 1963, Contract AF33(616)-8438

N63-20300-20-25, DS-119,
   M. Neuberger,
      "Silicon: Dielectric Constant Data Sheets,"
         January, 1963, Contract AF33(616)-8438

N63-20375-20-25, DS-118,
   M. Neuberger,
      "Silicon: Debye Temperature Data Sheets,"
         January, 1963, Contract AF33(616)-8438

N63-20717-21-09, NYU-TR400-81, AFCRL-63-317,
   G. J. Herskowitz,
      "Some Network Properties of the Large Area PN Junction, Fourth
      Scientific Report,"
         July, 1963, Contract AF19(628)-379

N63-20719-21-25, AFCRL-63-815,
   George Rupprecht,
      "The Surface Barrier Effect in Photovoltaic Conversion. Final
      Report,"
         May, 1963, Contract AF19(604)-8506

N63-21789-22-25, AMRA-TR63-03, MRL-130,
   D. R. Chipman, B. W. Butterman,
      "Contribution of Thermal Diffuse Scattering to Integrated Bragg
      Reflections from Perfect Crystals,"
         January, 1963

N63-21806-22-23, LMSC-6-90-62-35, SRB-62-41,
   J. B. Goldman,
      "Small Angle X-Ray Scattering: An Annotated Bibliography,"
         June, 1962

N63-22081-22-09, AFCRL-63-336,
   M. M. Atalla, et. al.,
      "Investigation of Hot Electron Emitter, Scientific Report No. 4,
      March 1, 1963 - May 31, 1963,"
         1963

N63-20205-20-25, AID-B-63-101,
   "Lattice Dynamics. Annotated Bibliography of Soviet Literature, 1962,"
      August 2, 1963

N63-22276-23-23, RFP-326,
   G. J. Werkema,
      "DRJXR.1: A Fortran Computer Program to Calculate Crystallographic
      D-Spacings and Bragg Angles,"

N63-22547-23-09, RADC-TDR-63-326,
   Hans J. Queisser,
      "Failure Mechanisms in Silicon Semiconductors,"
         August, 1963, Contract AF30(602)-3016

N63-22559-23-23, RSIC-65,
   J. G. Helmaks,
      "Theory and Practice of Electron Microscopic Stereophotography,"
         September 13, 1963

N63-22576-23-07, LMSC-SB-63-32,
   H. M. Abbatt, J. V. Kerrigan,
      "Epitaxial Growth: An Annotated Bibliography,"
         April, 1963

N63-22632-23-09, Q445-3,
   Egons Rasmanis, James Cline,
      "Active Thin-Film Techniques Micromin Program. Third Interim
      Development Report, December 23, 1962 - March 22, 1963,"
         April 14, 1963, Contract NObsr 87633

N63-22633-23-09, Q445-4,
   Egons Rasmanis, James Cline,
      "Active Thin-Film Techniques Micromin Program. Fourth Interim
      Development Report, March 23 - July 22, 1963,"
         August 20, 1963, Contract NObsr 87633

N63-22789-23-09,
   "Semiconductor Thin Films. Quarterly Report No. 6, April 1 - June 30,
   1963,"
      Contract AF33(657)-7623

N63-23084-24-25,
   "Research on Semiconductor Transport. Annual Summary Report, October 1,
   1962 - September 30, 1963,"
      Contract Nonr 2934(00)

N63-23353-24-01, SID-63-167,
  "Ultrasonic Cleaning; A Bibliography,"
    March 1, 1963

N63-23061-24-25,
  G. H. Wannier,
    "Dynamics of Block Electrons in Solids,"
      October 1, 1962, Contract Nonr 2771(05)

N64-10096-01-09, NASA CR-52190,
   S. A. Ring, J. B. Story,
      "Electrolytic Preparation of High Dielectric Thin Films. Quarterly
      Report, June 27, 1963 - September 27, 1963,"
         1963, Contract NASw-765

N64-10257-01-01, IS-700,
   "Annual Summary Research Report of Chemical Engineering, Metallurgy,
   Physics and Reactor Divisions. Annual Summary Report, July 1, 1962 -
   June 30, 1963,"
      September, 1963, Contract W-7405-eng-82

N64-10307-01-23,
   A. E. Spakowski,
      "Use of Polaroid Film in X-Ray Diffractions,"
         August, 1963

N64-10622-01-09, LS-BIB-63-3,
   C. L. M. Blocker, M. Bloomfield, T. J. Taylor,
      "Epitaxial Deposition of Semiconductor Materials: An Annotated
      Bibliography,"
         October, 1963

N64-10705-02-18, TRRS-17638,
   "Soviet Research in Rare Metal Industry,"
      February 14, 1963

N64-10708-02-25, JPRS-17689,
   "Translations from Fizika Tverdogo Tela (Solid State Physics)(Leningrad,
   V. 4) No. 7, 1962,"
      February 18, 1963

N64-10732-02-25, JPRS-18008,
   "Translations from Fizika Tverdogo Tela (Solid State Physics) No. 9,
   1962,"
      March 7, 1963

N64-10737-02-23, JPRS-18012,
   L. Belgagio,
      "Crystallography and Technology,"
         March, 1963

N64-10738-02-25, JPRS-18062,
   "Translations from Fizika Tverdogo Tela (Solid State Physics) No. 10,
   1962,"
      March 11, 1963

N64-11028-02-25, AD-423328,
   "Semiconductor Thin Films. Quarterly Report No. 7, July 1 - September 30,
   1963,"
      1963, Contract AF33(657)-7623

N64-11466-03-18,
   G. V. Samsonov, V. M. Sleptsov,
      "Preliminary Variant of the Phase Diagram of the Boron-Silicon
      System,"
         November 13, 1963

N64-11561-03-23, NASA-TTF-73,
   L. N. Dobretsov,
      "Electron and Ion Emission,"

N64-11923-03-15, JPRS-22443,
   Ye Ye Levin, V. M. Lukyanovich,
      "All-Union Conferences on Electron Microscopy and Nondestructive
      Methods of Testing,"
         December 24, 1963

N64-11933-03-25, AFCRL63-333, AD422580,
   S. S. Flaschen, H. W. Cooper, et. al.,
      "Research and Development for Surface Protection for Silicon Devices.
      Scientific Report No. 4, 15 December 1962 - 14 March 1963,"
         Contract AF19(604)-8358

N64-12095-03-07, EDR-3687,
   Charles Jirrell,
      "Survey of Applicable Electrochemical Technology, Operational and
      Fabrication Techniques and Materials,"
         December, 1963, Contract AT(30-1)-3101

N64-12237-03-15, AFCRL63-350,
   D. M. Jackson, Jr.,
      "Epitaxial Control System,"
         January 14, 1963, Contract AF19(604)-8351

N64-12590-04-25, RADC-TDR-63-443, AD-425472,
   H. Queisser, W. Shroen, et. al.,
      "Failure Mechanisms in Silicon Semiconductors,"
         November, 1963, Contract AF30(602)-3016

N64-12826-04-09, AD-422096,
   A. R. Von Hippel,
      "Progress Report No. XXXIII, Laboratory for Insulation Research,"
         July, 1963, Contracts Nonr-184(10), Nonr-184(88), AF19(628)-395,
         AF33(616)-8353, and AF19(604)-8483

N64-12998-04-09, AD-422536,
   W. Corrigan, et. al.,
      "Production Development of a Silicon Planar Epitaxial Transistor with
      a Maximum Operating Failure Rate of 0.001% per 1000 Hours at a Confi-
      dence Level of 90% at 25°C. Fourth Quarterly Report, February 1 -
      April 30, 1963,"
         Contract DA-36-039-SC86728

N64-13031-04-09, AD-424628,
   J. M. Blank, A. E. Cahill, et. al.,
      "Research on Thin Film Insulators. Second Interim Engineering
      Report,"
         October 25, 1963, Contract AF33(657)-11079

N64-13036-04-18, AD-423329,
   L. C. Kravitz,
      "ESR and Optical Experiments on Deep-Lying Impurities in Germanium
      and Silicon,"
         June 14, 1963, Contract Nonr-1866(10), Nonr-1866(16)

N64-13038-04-09,
   F. Tumbelty,
      "Production Engineering Measure of 2N 1708 Silicon Planar Epitaxial
      Transistor. Quarterly Report No. 5, May 1 - July 30, 1963,"
         Contract DA-36-039-SC-86729

N64-13075-04-09, AD-423673,
   S. J. Buginas,
      "Vacuum Disposition of Thin Film Electronic Components: An
      Annotated Bibliography,"
         February, 1963, Contract NOw-63-0050

N64-13636-05-25, ARL63-197, AD426752,
   E. L. Kern, D. E. Floyd, P. Bunce,
      "Low Energy Electron Diffraction from Single Crystal Surfaces I.
      Apparatus Design,"
         November, 1963, Contract AF33(657)-10798

N64-13784-05-25, RADC-TDR-63-464, AD-427117,
   G. Rapprecht,
      "Study of Surface States in Semiconductors,"
         December, 1963, Contract AF30(602)-3157

N64-13785-05-25, RADC-TDR-63-474, AD-427092,
   K. K. Beinhartz, V. A. Russell, et. al.,
      "Failure Mechanisms at Surfaces and Interfaces. First Interim
      Technical Documentary Report, July 1 - October 1, 1963,"
         December, 1963, Contract AF30(602)-3085

N64-13961-05-25, AD-427339,
   M. Lavik,
      "The Structure and Strength of Epitaxial Films. Bi-monthly Progress
      Report No. 1, October 17 - December 17, 1963,"
         January, 1964, Contract NOw-64-0061-d

N64-14019-05-07, AD-426742,
   Masey Bateman, et. al.,
      "Bibliography on Analytical Chemistry Relating to Borides, Carbides,
      and Nitrides of Group IV and V Elements,"
         1963, Contract DA-30-069-ORD-2787

N64-14022-05-25, AD-401398,
   H. C. Gatos, M. C. Lavine,
      "Chemical Behavior of Semiconductors: Etching Characteristics,"
         January 2, 1963, Contract AF19(628)-500-APRA-SD90

N64-14182-06-01, NAS-NRC-1139, AROD-3935.3, AD-424943,
   Daniel Berg, J. C. Devins,
      "Dielectrics: Digest of Literature, Vol. 26,"
         1962

N64-14295-06-25, RTD-TDR-63-4125, AD-427178,
   W. J. King, et. al.,
      "P-N Junction Formation Techniques, Third Quarterly Report, May 20 -
      September 1, 1963,"
         November, 1963, Contract AF33(657)-10505

N64-14504-06-09, AD-420958,
   R. M. Lichtenstein,
      "Investigation of Transient Radiation Damage in Semiconductor
      Materials,"
         1963, Contract DA-36-039-AMC-02165(E)

N64-14685-06-23, AFCRL-63-388, AD-428785,
   John O'Connor,
      "Analysis of Impurities in Solid State Electronic Materials, Final
      Report,"
         October 1, 1963, Contract AF19(604)-7463

N64-15339-07-07, ORNL-3537,
   M. T. Kelly, C. D. Susano,
      "Analytical Chemistry Division Annual Progress Report for Period
      Ending November 15, 1963,"
         February 18, 1964, Contract W-7405-eng-26

N64-15563-07-01,
   W. W. Blender,
      "Research Institute Far Advanced Studies, 1962, Summary of Year's
      Activities,"
         1962

N64-15687-07-07, SSD-TDR-63-349, TDR-269(4210-10)3, AD-429199,
   P. Breisache,
      "Mass Spectrometry and the Properties of Condensed Systems at High
      Temperatures,"
         December 27, 1963, Contract AF04-(695)-269

N64-16033-07-07, NASA CR-55774,
  "Solids Mass Spectrometer - First Quarterly Technical Progress Report,
    November 4, 1963 - February 3, 1964,"
      1964, NASA Contract NASn-839

N64-16216-08-23, JPRS-23510, OTS-64-21710,
  "X-Ray Diffraction Research,"
    March 4, 1964

N64-16434-08-23, ARL-63-246, AD-429228,
  Per-olov Lowdin,
    "Quantum Theory of Many-Particle Systems - Final Report, January 1,
      1960 - August 31, 1963,"
        September 30, 1963, Contract AF61(052)-351

N64-16739-08-25, NASA CR-53102, EE-4012-101-644,
  R. L. Ramey,
    "A Study of Thin Film Vacuum Deposited Junctions - (First) Annual
      Status Report, December 5, 1962 - December 5, 1963,"
        January, 1964, NASA Grant NSG-340

N64-16774-08-25, ESD-TDR-64-15, AD-429866,
  B. Lax, et. al.,
    "Solid State Quarterly Progress Report, Division 8 (October 1 -
      December 31, 1963,"
        February 6, 1964, Contract AF19(628)-500

N64-17618-09-25, NRL-MEMO-1432, AD-416457,
  C. O. Beachem, B. F. Frown, A. J. Edwards,
    "Characterizing Fractures by Electron Fractography. Part XII:
      Illustrated Glossary Section I: Quasi-Cleavage,"
        June, 1963

N64-17876-11-01, AD-431661,
  H. J. Zimmermann, G. G. Harvey,
    "Quarterly Progress Report No. 72 (Period Ending November 30, 1963)
    A Review of the Research Activities on Radio Physics, Plasma
    Dynamics, and Communication Sciences and Engineering,"
      January 15, 1964, NASA Grant NsG-496, Contracts DA-36-039-SC-
      78108 and AT(30-1-1842) and AF19(614)-5992, NSF(G-16526, et. al.

N64-18255-10-25, RADC-TDR-64-6, AD-434762,
  Queisser, Schroen, Hooper,
    "Failure Mechanisms in Silicon Semiconductors, Quarterly Report
      No. 3 (September 1 - November 30, 1963),"
        March, 1964, Contract AF30(602)-3016

N64-18259-10-07, ASD-TDR-63-620, AD-427027,
    M. Hoch,
        "Materials Analytical Research. Technical Documentary Report,
        June 15, 1960 - May 31, 1963,"
            November, 1963, Contract AF33(616)-7450

N64-18376-10-09, AL-TDR-64-29, AD-432171,
    R. M. Burger,
        "Selected Experiments in Silicon Integrated Device Technology
        (Final Report, January, 1963 - February, 1964),"
            March, 1964, Contract AF33(657)-10340

N64-18592-11-25, R63ELS-74, RADC-TDR-64-35, AD-435469,
    K. K. Reinhartz, V. A. Russell, et. al.,
        "Failure Mechanisms at Surfaces and Interfaces, Second Interim
        Technical Documentary Report, October 1, 1963 - January 1, 1964,"
            March, 1964, Contract AF30(602)-3085

N64-18638-11-25, NLCO-903,
    P. R. Morris,
        "The Inversion of Pole Figures for Materials Having Orthorhomhic
        Symmetry,"
            April 10, 1964, Contract AT(30-1)-1156

N64-18657-11-25, Report 51, AD-429325,
    J. C. Slater, M. P. Barnett, et. al.,
        "Solid State and Molecular Theory Group, Quarterly Progress Report,"
            January 15, 1964, Contract Nonr-1841(34), NSF Grants 24908 and
            10821, AF19(628)-356

N64-18880-11-23, PIBMRI-1008-62, AFCRL-62-166, AD-286308,
    T. Tamir, A. A. Olines
        "Guided Complex Waves. Part I. Fields at an Interface,"
            March 21, 1962, Contract AF19(604)-7499

N64-18941-11-23, AFCRL-63-325(2), AD-435620,
    A. Kohan,
        "On Determination of the Optical Absorption Coefficient, II,"
            December, 1963

N64-18960-11-25, NASA-TN-2275,
    R. J. Bacigalupie,
        "Surface Topography of Single Crystals of Face-Centered-Cubic,
        Body-Centered-Cubic, Sodium Chloride, Diamond, and Zinc-Blende
        Structures,"
            April, 1964

N64-19018-11-25, LA-3043,
    A. C. Larsan, D. T. Cromer,
        "An Integrated Series of Crystallographic Computer Programs II.
        Processing Collected Intensity Data,"
            April 17, 1964, Contract W-7405-eng-36

N64-19550-12-25, AD-434381,
    A. C. Zittlemayer, K. D. Iyengar, W. M. Block,
        "Studies of the Surface and Corollary Electrical Properties of
          Germanium, Final Report, April 16, 1961 - February 29, 1964,"
          1964, Grant DA-SIG-36-039-61-G5

N64-19591-12-09, NASA CR-53841,
    D. R. Corley, R. Rosenzweiz,
        "Design, Development and Fabrication of a Fast Silicon Power
          Transistor, Summary Report, May 28, 1962 - August 28, 1963,"
          1963, NASA Contract NAS8-5006

N64-19824-12-23, NASA CR-53878,
    L. J. Frisco,
        "Investigation of the Behavior of Dielectric Materials at High
          Field Strengths in a High Vacuum Environment, First Quarterly
          Report, April 1 - June 30, 1963,"
          July 11, 1963, NASA Contract NAS8-5253

N64-19939-12-24, NASA CR-53929, JPL-TR-32-515,
    Douglas B. Nash,
        "Nelo Technique for Quantitative SiO_2 Determination of Helical
          Materials by X-Ray Diffraction Analysis of Glass,"
          July 27, 1963, NASA Contract NAS7-100

N64-20275-13-23, D1-82, 0169-R1, AD-428452,
    Regis M. N. Pelloux,
        "The Analysis of Fracture Surfaces by Electron Microscopy,"
          December, 1963

N64-20334-13-9, USAELRDL-TR-2333, AD-408131,
    B. Reich, E. B. Hakim,
        "Bulk Reliability Effects in Semiconductor Devices; Current Crowding
          in Transistors,"
          February, 1963

N64-20397-13-25, RTD-TDR-63-4145, AD-428995,
    F. N. Hodgson, J. E. Katon,
        "Studies in Solid State Mass Spectrometry, Technical Documentary
          Report, July 1, 1962 - July 1, 1963,"
          December, 1963, Contract AF33(616)-8465

N64-20453-13-23, AD-435880,
    R. A. Smith, et. al.,
        "Research in Materials Sciences and Engineering, Annual Report No.
          3, 1963-1964,"
          April, 1964, Contracts ARPA-SD90; DA-19-020-AMC-0231(X);
          Nonr 184(10);AF04(694)-305; AT(10-1)-1067, et. al.

N64-20639-13-15, NASA CR-56015,
    E. S. Machlin,
        "A Field Ion Microscope Facility for Solid State and Surface Studies,"
        March 31, 1964, NASA Grant NsG-294-63

N64-20642-13-15, NASA CR-56039,
    "Solids Mass Spectrometer, Quarterly Technical Progress Report No. 2,
    February 4 - May 3, 1964,"
        1964, NASA Contract NASw-839

N64-20690-13-24, NASA CR-56103,
    M. K. Testerman, et. al.,
        "Basic Experimental Research Leading to Improved Cold Electron Sources
        and New Types of Velocity Filter Mass Spectrometers, Final Report
        (April 10, 1964),"
            Grant NsG-153-61

N64-20967-14-09,
    M. F. Goldberg,
        "Physics of Failure in Electronics Vol. 2 (Proc. Second Annual
        Symposium on the Physics of Failure in Electronics),"

N64-21086-14-07, RTD-TDR-63-4128, AD-428014,
    G. D. Perkins,
        "Mass Spectrometer Output Interpretation, Technical Documentary
        Report, April 1, 1962 - October 31, 1963,"
            October, 1963, Contract AF33(657)-8174

N64-21148-14-09, SB-64-2, Report 3-35-64-2, AD-600708,
    J. B. Goldmann,
        "Printed Circuits and Welded Modules (1963); An Annotated Bibliography,"
            December, 1963, Contract AF04(647)-673

N64-21725-15-25, AFCRL-64-360, AD-600799,
    S. P. Wolsky,
        "Investigation of Ultra High Vacuum Sputtered Thin Films, Scientific
        Report No. 1,"
            May, 1964, Contract AF19(628)-3840

N64-21769-15-25, MEMO-400, AD-428846,
    P. G. Sedlewicz, R. E. Onley, C. R. Kannewurf,
        "Electron and Hole Injection by a Metal-Depletion Layer Contact,"
            December 30, 1963, Contract NOw-62-0749-D

N64-21832-15-25, RTD-TDR-63-4264, AD-433828,
    E. Krikorian, R. S. Sneed, et. al.,
        "Vacuum Evaporated and Cathodic Sputtered Thin Films,"
            March, 1964, Contract AF33(657)-8728

N64-21953-15-25, FTD-TT-63-687/1+2, AD-428315,
   E. M. Omel'yanovskiy, et. al.,
      "Mobility of Electrons in Highly Alloyed Silicon,"
        1963

N64-21967-15-15, FTD-TT-62-1863/1+2+4, AD-421460,
   A. A. Korsuwskiy, I. G. Razumnov,
      "A Thickness Monitor for Thin Films Obtained by Vacuum Spraying,"
        1960

N64-22222-15-25, ESD-TDR-64-16, AD-435023,
   "Solid State Research, 1963,"
      March 9, 1964, Contract AF19(628)-500

N64-22278-15-09, RADC-TDR-64-111, AD-600875,
   "Detailed Study of Deleterious Effects on Silicon Transistors,"
      April, 1964, Contract AF30(602)-3244

N64-22505-15-19, AD-600316,
   S. W. Chaikan, G. A. St. John,
      "Dielectric Thin Films with Increased Breakdown Strength,"
        April 15, 1964, Contract DA-36-039-SC-B7460

N64-22530-15-25, Q445-7, AD-601021,
   E. Rusmanis, J. Cline, R. Tierman,
      "Active Thin Film Techniques Micromin Program, Interim Development
      Report No. 7, February 1 - April 30, 1964,"
        May 28, 1964, Contract NObsr-87633

N64-22612-15-23, AFCRL-64-383, AD-441461,
   W. W. Hunt, Jr.,
      "Charge Transfer Studies with a Time-of-Fight Mass Spectrometer: II
      Kinetic Analysis Including Attenuation of Both Neutrals and Ions by
      Scattering, Physical Sciences Research Paper No. 16,"
        May, 1964

N64-22762-16-07, NASA CR-50678,
   K. Biemann,
      "The Detection and Identification of Organic Matter by Mass
      Spectrometry, Second and Third Semiannual Report, January 1, 1962 -
      May 31, 1963,"
        1963, Grant NsG-211-62

N64-22897-16-25, ML-1131, AD-431112,
   R. H. Pantell, M. DiDomenico,
      "The Theory of Direct Transitions in Semiconductors,"
        1964, Contract Nonr-225(48)

N64-23176-16-25,
   M. J. Bloom,
      "Solid State Bonding,"
        1964

N64-23290-16-19, FTD-TT-62-1709/1+2, AD-401734,
    S. M. Stishov, N. V. Belov,
        "Crystalline Structure of the New Close-Grained Modification of
        Silica, SiO_2,"
            February 13, 1963

N64-23883-16-09, SB-62-67, Report 3-35:62-8, AD-410235,
    J. B. Goldmann,
        "Microminaturization; Its Application to Electronic Circuits and
        Components: An Annotated Bibliography,"
            June, 1963, Contract AF04(647)-787

N64-23957-16-09, RADC-TDR-64-125, AD-601819,
    "Failure Mechanisms in Microelectronics, Third Quarterly Report,"
        May, 1964, Contract AF30(602)-3017

N64-23960-16-09, RADC-TDR-64-153, AD-601820,
    W. Schroen, W. W. Hooper, H. J. Queisser,
        "Failure Mechanisms in Silicon Semiconductors, Fourth Quarterly
        Report, November 30, 1963 – February 29, 1964,"
            May, 1964, Contract AF39(602)-3016

N64-24199-16-16, AD-417763,
    R. C. Willson,
        "The Theory, Design, and Development of An Interferometric
        Spectrometer, Scientific Report No. 1 and 2, January, 1962,
        June, 1963,"
            July 1, 1963, Contracts AF19(604)-7240, AF19(628)-287

N64-24787-17-23, NASA CR-84,
    P. J. Bryant, C. M. Gosselin,
        "Extreme Vacuum Technology (Below 10^{-13} Torr) and Associated Clean
        Surface Studies,"
            July, 1964, Contract NASr-63(06)

N64-25320-17-25, SAR-8, AD-439958,
    L. N. Hadley,
        "Studies, Research, and Investigations at the Optical Properties of
        Thin Films of Metal Semiconductors and Dielectrics, Semi-annual
        Report, February 16 – August 15, 1963,"
            1963, Contract DA-44-009-eng-3828

N64-25624-17-09, TRI, AD-439341,
    R. A. Horn,
        "Theory of Electrical Conductance in Acidic Aqueous Solutions,"
            May 15, 1964, Contract Nonr-4424(00)

N64-25751-17-23, A046-F, AD-602043,
  J. P. Spatt,
      "Thin Film Active Devices Final Report, June 22 - September 30, 1963,"
          February 20, 1964, Contract DA-49-186-ORD-1056

N64-25976-18-25, AFCRL-64-278, AD-600725,
  E. B. Dale, G. Senecal, et. al.,
      "The Preparation and Properties of Thin Films of Semiconductors,"
          March 1, 1964, Contract AF19(604)-7218

N64-26012-18-09, NAVWEPS-8190, AD-600676,
  G. G. Kretschman, R. F. Potter,
      "Techniques and Apparatus for Evaporating Compound Semiconductors,"
          April 1, 1964

N64-26230-18-25, NOLTR-64-30, AD-442905,
  W. W. Scanlon,
      "Solid State Research for the Year 1963,"
          February 17, 1964

N64-26273-18-25, AD-440163,
  E. L. Lind, E. R. Hill, D. H. Dickey,
      "Study of Photoconductivity in Thin Films, Interim Engineering
      Report, November 1 - May 1, 1963,"
          May 15, 1964, Contract AF33(615)-1090

N64-26264-18-25, ESD-TDR-64-47, AD-439365,
  A. McWhorter, P. E. Tannenwald,
      "Solid State Division 8 Quarterly Progress Report, January 1 -
      March 31, 1964,"
          May 5, 1964, Contract AF19(628)-500

N64-26487-18-07, DP-879,
  J. A. Wheat,
      "Determination of Metallic Impurities in Water by Atomic Absorption
      Spectrometry,"
          June, 1964, Contract AT(07-2)-1

N64-26649-18-25, AD-439686,
  "Solid State Research, 1963, No. 2,"
      August 16, 1963, Contract AF19(628)-500

N64-26898-18-25, AFCRL-64-564, AD-603090,
  P. T. Landsberg, D. A. Evens,
      "Research on Recombination Fluctuation Theory in Semiconductors,
      Scientific Report No. 1, February, 1963 - April 30, 1964,"
          May 31, 1964, Contract AF61(052)-664

N64-26918-18-25, RADC-TDR-64-138, AD-603279,
    K. F. Greenough,
        "Failure Mechanisms at Metal-Dielectric Interfaces,"
            July, 1964, Contract AF30(602)-3266

N64-26919-18-25, RADC-TDR-64-168, AD-603262,
    G. Rupprecht, J. Gilbert,
        "Study of Surface States in Semiconductors,"
            July, 1964, Contract AF30(602)-3157

N64-27216-19-25, AROD-2178-8, AD-443952,
    C. S. Barrett,
        "Diffraction Studies of Crystal Imperfections, Final Report, July 1,
        1961 - June 30, 1964,"
            June 30, 1964, Grant DA-ARO(D)-31-124-G(52)

N64-27235-19-25, SMIR-63-3, AD-437866,
    E. J. Soxman, G. N. Steele,
        "Thin Film Research,"
            November 4, 1963, Contract Nonr-4165(00)

N64-27344-19-25, AD-439233,
    "Semiconductor Research, Semiannual Report, October 1, 1963 - March 31,
    1964,"
        1964, Contract DA-31-124-ARO(D)-17

N64-27425-19-25, ARL-64-98,
    W. R. Rambauske,
        "Optical Properties of Semiconducting Crystals,"
            June, 1964, Contract AF33(616)-7500

N64-27928-20-25,
    P. Wong, B. Selikson, et. al.,
        "Development of Epitaxial Technology for Microelectronics and Large
        Area Device Application, Quarterly Report, February 1 - April 30,
        1964,"
            June 1, 1961

N64-28579-20-25, AFCRL-64-467, AD-603783,
    H. H. Woodbury, M. Avea, et! al.,
        "Semiconductor Device Concepts, Scientific Report No. 7,"
            May 5, 1964, Contract AF19(628)-329

N64-28667-20-25,
    J. W. Allen,
        "Theory of Energy Levels of Transition Metal Impurities in Semi-
        conductors,"
            July, 1964

N64-28765-20-25, ARPA SD-67, AR-4, AD-602012,
   "Materials Research Center 1963-64 Annual Report, Fourth Annual Report,
   May 1, 1963 - January 31, 1964,"
      1964

N64-28888-20-08, NASA CR-58597,
   J. Lederberg,
      "Computation of Molecular Formulas for Mass Spectrometry,"
         1964, Grants NsG-81-60, NSF G-6411, NIH G-NB-04270-01,
         NIH G-NB-04270-02, NIH G-AI-5160-06

N64-28961-20-10,
   M. Lauriente, C. A. Harper, et. al.,
      "Planar Integration of Thin Film Units, First Quarterly Progress
      Report, January 15 - April 14, 1964,"
         1964

N64-29186-21-07, NASA CR-58503,
   A. E. Hultquist, M. E. Sibert,
      "Electrolytic Preparation of High Dielectric Thin Films, Annual
      Report, June 27, 1963 - June 27, 1964,"
         1964, Contract NASw-765

N64-29563-21-09, NASA CR-56796,
   M. K. Testerman, B. E. Gilliland, E. M. King,
      "A Cold Electron Mass Spectrometer Ion Source,"
         1964, Grant NsG-260-62

N64-29398-21-23, SAR-9, AD-445110,
   L. N. Hadley,
      "Studies, Research, and Investigations of the Optical Properties
      of Thin Films of Metal: Semiconductors and Dielectrics, Semi-
      annual Report, August 16, 1963 - February 15, 1964,"
         1964, Contract DA-44-009-eng-3828

N64-29700-21-15, NASA CR-58538,
   "Solids Mass Spectrometer, Quarterly Technical Progress Report No. 3,
   May 4 - August 3, 1964,"
      1964, Contract NASw-839

N64-29929-21-25, AMRL-TDR-63-117, AD-604419,
   K. K. Knaell, M. O. Thurston,
      "Investigation of New Semiconductor Phenomenon,"
         June, 1964, Contract AF33(606)-8384

N64-29967-21-25, RADC-TDR-64-197, AD-604349,
   K. K. Reinhantz, et. al.,
      "Failure Mechanisms at Surfaces and Interfaces, Third Interim
      Technical Documentary Report, January 1 - April 1, 1964,"
         July, 1964, Contract AF30(602)-3085

N64-30006-21-25, AROD-3330-4, AD-604660,
  R. K. Gereth, et. al.,
    "Research on the Influence of Surface Conditions on Diffusion in
    Silicon, Final Report, June 16, 1961 - June 15, 1964,"
      July, 1964, Contract DA-04-200-ORD-1166(X)

N64-30123-21-25, AFCRL-64-581, AD-605566,
  K. D. Kang, F. Lee, H. W. Cooper,
    "Research and Development for Semiconductor Surface Control and
    Stabilization, Scientific Report No. 1,"
      May 14, 1964, Contract AF19(628)-3808